HIGH RESOLUTION TSUNAMI VULNERABILITY ASSESSMENT BY GIS-BASED MULTI-CRITERIA DECISION MAKING ANALYSIS AT YENİKAPI, İSTANBUL

A THESIS SUBMITTED TO
THE GRADUATE SCHOOL OF NATURAL AND APPLIED SCIENCES
OF
MIDDLE EAST TECHNICAL UNIVERSITY

BY

ZEYNEP CEREN ÇANKAYA

IN PARTIAL FULFILLMENT OF THE REQUIREMENTS
FOR
THE DEGREE OF MASTER OF SCIENCE
IN
GEOLOGICAL ENGINEERING

JANUARY 2015

Approval of the thesis:

HIGH RESOLUTION TSUNAMI VULNERABILITY ASSESSMENT BY GIS-BASED MULTICRITERIA DECISION MAKING ANALYSIS AT YENİKAPI, İSTANBUL

submitted by **ZEYNEP CEREN ÇANKAYA** in partial fulfillment of the requirements for the degree of **Master of Science in Geological Engineering Department, Middle East Technical University** by,

Prof. Dr. Gülbin Dural Ünver
Dean, Graduate School of **Natural and Applied Sciences** _____

Prof. Dr. Erdin Bozkurt
Head of Department, **Geological Engineering** _____

Prof. Dr. M. Lütfi Süzen
Supervisor, **Geological Engineering Department, METU** _____

Prof. Dr. Ahmet Cevdet Yalçıner
Co-Supervisor, **Civil Engineering Dept., METU** _____

Examining Committee Members

Prof. Dr. Erdin Bozkurt
Geological Engineering Dept., METU _____

Prof. Dr. M. Lütfi Süzen
Geological Engineering Dept., METU _____

Prof. Dr. Ahmet Cevdet Yalçıner
Civil Engineering Dept., METU _____

Assist. Prof. Dr. A. Arda Özacar
Geological Engineering Dept., METU _____

Dr. Işıkhan Güler
Civil Engineering Dept., METU _____

Date: 23.01.2015

I hereby declare that all information in this document has been obtained and presented in accordance with academic rules and ethical conduct. I also declare that, as required by these rules and conduct, I have fully cited and referenced all material and results that are not original to this work.

Name, Last name: Zeynep Ceren ÇANKAYA

Signature :

ABSTRACT

HIGH RESOLUTION TSUNAMI VULNERABILITY ASSESSMENT BY GIS-BASED MULTICRITERIA DECISION MAKING ANALYSIS AT YENİKAPI-İSTANBUL

Çankaya, Zeynep Ceren

M.S., Department of Geological Engineering

Supervisor: Prof. Dr. M. Lütfi Süzen

Co-Supervisor: Prof. Dr. Ahmet Cevdet Yalçıner

January 2015, 94 pages

İstanbul is a mega city with its various coastal utilities located at the northern coast of the Sea of Marmara. At Yenikapı, there are critical vulnerable coastal utilities, structures and active metropolitan life. Fishery ports, commercial ports, small craft harbors, passenger terminals of intercity maritime transportation, water front commercial and/or recreational structures with residential/commercial areas and public utility areas are some examples of coastal utilization which are vulnerable against marine disasters. Therefore, tsunami vulnerability of Yenikapı region is an important issue of İstanbul.

In this study, a new methodology of hazard analysis for areas under tsunami attack is proposed, where Yenikapı region is chosen for a case study. Available datasets of İstanbul Metropolitan Municipality (IMM) and Turkish Navy are used as inputs for high resolution GIS-based MCDA assessment of tsunami hazard in Yenikapı. Bathymetry and topography database is used for high resolution tsunami numerical modeling where the tsunami parameters from deterministically defined worst case

scenarios are computed from simulations using tsunami numerical model NAMI DANCE. In order to define tsunami vulnerability of the region, two aspects vulnerability at location and evacuation resilience maps were created using AHP method of MCDA. Vulnerability map is composed of metropolitan use, geology, elevation, and distance from shoreline layers, whereas the evacuation resilience layer is formed by slope, distance within flat areas, distance to buildings and distance to road networks layers. The tsunami hazard map is then computed by proposed new relation which uses flow depth map, vulnerability at location map and evacuation resilience maps.

Keywords: Tsunami Vulnerability Assessment, Geographic Information Systems (GIS), Multicriteria Decision Making Analysis (MCDA), Analytical Hierarchical Model (AHP), Tsunami Hazard Analysis (THA)

ÖZ

COĞRAFİ BİLGİ SİSTEMİNE DAYALI ÇOK ÖLÇÜTLÜ KARAR ANALİZİYLE YÜKSEK ÇÖZÜNÜRLÜKLÜ TSUNAMİ HASAR GÖREBİLİRLİK ANALİZİ: YENİKAPI-İSTANBUL

Çankaya, Zeynep Ceren

Yüksek Lisans, Jeoloji Mühendisliği Bölümü

Tez Yöneticisi: Prof. Dr. M. Lütfi Süzen

Ortak Tez Yöneticisi: Prof. Dr. Ahmet Cevdet Yalçıner

Ocak 2015, 94 sayfa

Mega şehir İstanbul, tüm kıyılarında çeşitli tesislerle donatılmıştır. Yenikapı Bölgesi'nde, önemli oranda hasargörebilir kıyı yapılarının yanısıra, büyükşehire özgü ciddi bir hareketlilik - aktif bir yaşam vardır. Bu bölge de; ticari liman, balıkçı limanı, yolcu terminali, ticari ve kamusal rekreasyon alanları ile önemli kıyı merkezlerinden biri olup, bu alanlar tsunamiye karşı hasar görebilir durumdadır. Bu nedenlere bağlı olarak Yenikapı Bölgesinin tsunami etkilerine karşı hasar görebilirlik analizi yapılması yararlıdır.

Bu çalışmada, tsunami etkisi altında hasar görebilirlik analizi için yeni bir yöntem Yenikapı bölgesine uygulanarak önerilmiştir. Çalışmada, İstanbul Büyükşehir Belediyesi'nin (İBB) ve Deniz Kuvvetleri verileri girdi olarak kullanılmış ve yüksek çözünürlüklü bir model oluşturulmuştur. Yüksek çözünürlüklü sayısal tsunami modellemesi için çalışma alanına ait batimetri ve topografya veri tabanları

kullanılmıştır. Deterministik olarak belirlenmiş en kötü durum senaryolarına ait tsunami parametreleri, sayısal tsunami modeli NAMI DANCE benzetimleriyle hesaplanmıştır. Hasar görebilirlik parametreleri, konum nedeniyle hasar görebilirlik ve tahliye esnekliği olarak iki gruba ayrılmıştır. Oluşturulan bu parametreler CBS tabanlı Çok Ölçütlü Karar Analizi (ÇÖKA) kullanarak üretilmiş ve incelenmiştir. Metropolitan kullanım şekli, jeoloji, denizden yükseklik ve kıyı şeridinden uzaklık katmanlarından hasar görebilirlik haritası; eğim, düz alana mesafe, binalara olan uzaklık ve yol ağına olan uzaklık katmanlarından tahliye esnekliği haritası üretilmiştir. Tsunami tehlike haritaları, tsunami kaynaklı su yüksekliği, hasar görebilirlik ve tahliye esnekliği haritalarını ilişkilendiren yeni bir denklemde hesaplanarak sunulmuştur.

Anahtar Kelimeler: Tsunami Hasar Görebilirlik Değerlendirmesi (THD), Coğrafi Bilgi Sistemleri, Çok Ölçütlü Karar Analizi (ÇÖKA), Analitik Hiyerarşi İşlemi (AHİ), Tsunami Tehlike Analizi (TTA)

To my beloved family,

ACKNOWLEDGEMENTS

First and foremost, I feel gratitude to my supervisor, Prof. Dr. M. Lütfi Süzen, to support me for this study. I would like to thank to him for his patience, motivation and immense knowledge. I am grateful to him for the long discussions that helped me sort out the technical details of my work. I am also thankful to him for encouraging the use of correct grammar and consistent notation in my writings and for carefully reading and commenting on countless revisions of my writing.

I would like to express my deepest gratitude to my advisor, Prof. Dr. Ahmet Cevdet Yalciner, for his excellent guidance, caring, patience, enthusiasm and providing me with an excellent atmosphere for doing this thesis. I feel gratitude him to give me the opportunity to not only be a part of the Coastal and Ocean Engineering Laboratory's precious family, but also always motivate me for finalizing my thesis. I attribute the level of my Master's degree to his encouragement and effort and without him this thesis, too, would not have been completed or written. One simply could not wish for a better or friendlier co-supervisor. I like his perspective on life such as living on the edges with balance and enjoying the life. He never push you find what we desire by myself

Besides my supervisor and co-supervisor, I would also thank to the other members of my thesis committee because of their guides to me through last one year. Thank you to Prof. Dr. Erdin Bozkurt, Assist. Prof. Arda Özacar and Dr. Işıkhan Güler for being my major advisors and making lots of effort to move this study forward with their constructive criticism and comments.

I am so grateful to have this opportunity for working with Dr. Çağıl Kolat. The impact of her to my study is obviously indisputable. Since my undergraduate studies, she has been a guided spirit to me. I learned many things from her and she endeavor to develop this dissertation.

I would like to special thank Betül Aytöre, a good friend, was always willing to help and to give her best suggestions. It would definitely have been in a lonely lab and suffering thesis period without her. She was always there to enlighten me with her knowledge and practical solutions. She always inspired me in all aspect of life and she has been my confidant, pillar of support and joy of my life during the long and though period of this dissertation.

I am also deeply thankful to Cem Ünüştü. His contributions to my study cannot be forgotten. He was always there whenever I need his support since the beginning. His knowledge and capability always guided me to improve my knowledge. I would also thank to his lovely and cheerful wife, Cansu Ünüştü, for her food feasts.

I am deeply grateful to my dearest 'Suzy', Müge Ergene, for providing me with unfailing support and continuous encouragement throughout my years of study. Whenever I felt desperate, she was there to and through the process of revisions of my thesis. She endeavor and spend her long time for helping me.

I am also deeply grateful to Nazlı Akkaş, for her contribution and psychological supports during my thesis period. She always stands next to me and ready for help in any condition. She never let me leave to complete this dissertation and motivate me by always being cheerful, understanding and helpful.

I would like to thank to my Deputy General Manager, Mr. Nedim Serkan Gür, because of his understanding, toleration and support during writing period of my thesis.

I would like to thank specially to my tolerant, sympathizer and helpful colleagues Faik Uçkan and İnci Demirtaş and her warm-hearted husband, Gökhan Demirtaş, for believing me and supporting me to finalize this dissertation.

I would like to present my special thanks to Çağdaş Bilici who shared his room with me and always believed in me, and Gökhan Güler, who was always ready for helping me when I freaked out because of my thesis.

I am deeply thankful to the members of GANG, Sailaja Prasad Mohanty and Magda

Szostek for their continued support and encouragement. They surround me with funny faces and they contribute cheer to my life with their existence. Especially Mohanty spent some time to read my thesis and correct my mistakes.

I would like to thank Alev Özen, Seda Uçar, Zeynep Deniz Erdoğan, Sercan Cihanbilir, Ezgi Nazlıbilek, Özge Koca, Gökhan Bektaş, Mert Pülten, Elif Marakoğlu, Pınar Berberoğlu and Miran Dzabic for sharing joyful moments with me throughout my long thesis period.

I would like to thank each member of TiyatroMUZ, amateur drama group, for their psychological support and encouragement to finalize my study. The last 2-3 months before completion of my thesis, I feel so peaceful and blessed with a friendly and cheerful group of people.

Most importantly, none of this would have possible without the love and patience of my family. My immediate family, to whom this dissertation is dedicated to, has been a constant source of love, concern, support and strength all these years. For this reason, I would like to express my heart-felt gratitude to Handan and Osman Çankaya, my parents, and Seren Çankaya, my sister. It would be an understatement to say that, as a family, we have experienced some ups and downs in the past three years. Every time, I was ready to quit, but you did not let me and I am forever grateful. This dissertation stands as a testament to your unconditional love and encouragement. I would also thank to my extended family for their aid and encouragements throughout this endeavor. I would like to special thanks to my grandmother, Ayla Tan. With her own brand of humor, she has been kind and supportive to me over the last several years.

TABLE OF CONTENTS

LIST OF TABLES

LIST OF FIGURES

LIST OF SYMBOLS AND ABBREVIATIONS

AHP	*: Analytical Hierarchical Model*
DEM	*: Digital Elevation Model*
DFZ	*: Dead sea Fault Zone*
EAFZ	*: East Anatolian Fault Zone*
GIS	*: Geographical Information Systems*
IMM	*: İstanbul Metropolitan Municipality*
MCDA	*: Multicriteria Decision Making Analysis*
MSZ	*: Makran Subduction Zone*
MWL	*: Mean Water Level*
NAF	*: North Anatolian Fault*
NAFZ	*: North Anatolian Fault Zone*
SWL	*: Sea Water Level*
PIN	*: Prince's Island Normal Fault*
PTVA	*: Papathoma Tsunami Vulnerability*
PTVAM	*: Papathoma Tsunami Vulnerability Assessment Model (PTVAM).*
TNM	*: Tsunami Numerical Modeling*
TVA	*: Tsunami Vulnerability Assessment*
USGS	*: The U.S. Geological Survey*
WLC	*: Weight Linear Combination*
YAN	*: Yalova Normal Fault*

CHAPTER 1

INTRODUCTION

Tsunamis are the giant waves mostly triggered by earthquakes and/or submarine landslides. Despite of rare occurrence of tsunamis, they have been of interest to the worldwide media since the early 21st century with the repetition of mega earthquakes (Cartwright and Nakamura, 2008, Mas et al., 2014). There are many associations researching and developing models to be able to forecast tsunamis and create tsunami inundation and evacuation maps in all over the world. The scientific and technical approach for the tsunami risk assessment has been developing in every day.

In last two decades, there is a considerable rise in the studies related with the hazard, risk and vulnerability (Alexander, 2000; Wisner et al., 2004). Many models have been developed to understand, assess and map these three concepts (Fischer et al., 2002; Gambolati et al., 2002; Cheung et al., 2003). The validation of the models is required in order to make the accurate estimation which is close to the real-world by modeling. The requisite of validation of hazard, risk and vulnerability models is because of the usage of the outputs to define land use zoning and planning, emergency response action, disaster planning, and insurance premiums (Tüfekçi, 1995, Jenkins 2000; Dominey-Howes and Papathoma, 2006). Recently, Geographic Information System (GIS) frameworks are used for vulnerability assessment models for many types of natural hazard.

Starting with the 2004 Indian Ocean tsunami, different methodologies have been developed to evaluate vulnerability to various types of natural hazards, including tsunamis (Papathoma et al., 2003; Ghobarah et al., 2006; Dominey-Howes & Papathoma, 2007; Reese et al., 2007; Taubenbock et al., 2008; Dall'Osso et al, 2009;

Wood, 2009; Pendleton et al., 2010; Atillah et al., 2011; Leone et al, 2011; Murthy et al., 2011; Sinaga et al., 2011; Eckert et al., 2012; Ismail et al., 2012; Usha et al., 2012) as cited in Santos et al., 2014. In order to create appropriate models for hazard assessments, the use of GIS tools is required for analyzing the hundreds of data and generating maps. The integration of various data can be performed and the results obtained from models can be presented as integrated with spatial and thematic data of selected region. Because of the easiness of data integration, many researchers preferred to use analytical GIS tools for the hazard modeling. In coherence with this approach, GIS tools are used in this study for further generating hazard models while analyzing and visualizing the results of numerical models.

This study is consisted of 5 chapters. Chapter 1 continues with the determination of purpose and scope, and the selected study area. Chapter 2 is dedicated to the simulations performed by tsunami numerical modeling. Chapter 3 focuses on the tsunami vulnerability and hazard assessment at Yenikapı region. Chapter 4 is devoted to the discussion of the obtained results for Yenikapı region. The study is completed with Chapter 5 which lists the conclusions of this study and the suggestions for future studies.

1.1 Purpose and Scope

The aim of this study is to develop (i) a new approach and methodology for GIS-based Tsunami Vulnerability Assessment (TVA) by using high resolution (1 m) GIS based data in tsunami numerical modeling and inundation analysis, and (ii) proposing a hazard assessment method considering locational vulnerability and evacuation resilience and the result of high resolution numerical models in Yenikapı region in İstanbul.

The possible tsunami sources in the Sea of Marmara have been evaluated and reasonable worst case is selected from available reports and literature. The tsunami numerical model NAMI DANCE is used for simulation and assessment of tsunami inundation and tsunami interaction with the metropolitan structures.

1.2 Study Area

1.2.1 The Sea of Marmara and Yenikapı

Besides amazing historical places and gorgeous nature of Turkey, it has a crucial geopolitical position and economically significant places. Turkey is surrounded by seas in three sides and is shaped by active faults, resulting in an inevitable interaction yielding tsunami potential. Some of those active faults are in the Sea of Marmara. İstanbul is one of the most important metropolitan cities in the world, which is located near to the faults in the Sea of Marmara. Based on Altınok et al., (2011), there were more than 134 tsunamis impacting on and around coasts of Turkey from 17th century BC to 1999 AD. Those tsunamis were triggered by earthquakes and/or submarine landslides.

The Sea of Marmara is an inland sea which connects the Black Sea to the Aegean Sea, and also separates Asia from Europe. It is connected to the Black Sea by the Bosphorus strait and to the Aegean Sea by the Dardanelles. It occupies an area with the approximate dimensions of 275 km (E-W direction) and 80 km (N-S direction). The maximum depth reaches around 1200 meters; it is a large-scaled intercontinental sea (Smith et al., 1995; Yalciner et al., 2002.)

The locations of the historical tsunamis (AD 120-1999) in the Sea of Marmara are shown in Figure 1 which the numbers are in chronological order. The figure is taken from Yalciner et al., (2002), where the seismotectonic map was modified from Yaltırak et al., (2000).

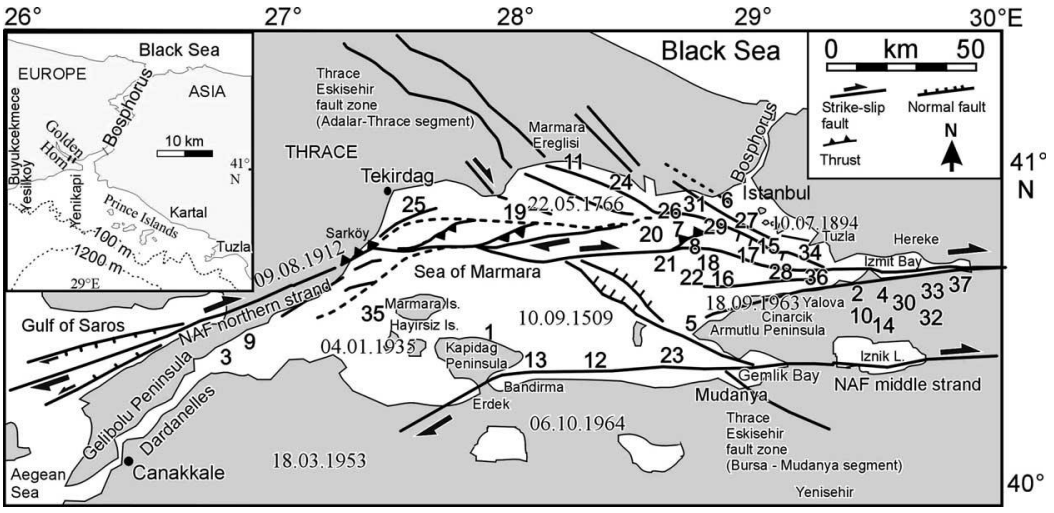

Figure 1: The seismotectonic map and the locations of the past tsunamis in the Sea of Marmara (Yalciner et. al., 2002)

Yenikapı, which is in Fatih district, is located at southern part of Haliç European side of İstanbul (Figure 2). One of the ancient city walls of İstanbul is located at the Yenikapı coast. Yenikapı station hosts a suburban railway, subway line, undersea railway connection (Marmaray) between Europe and Asia. The entrance of the Eurasia Undersea Highway Tunnel at Europe side is also located near the coast of Yenikapı.

Figure 2: Google Earth image of the study area, Yenikapı, İstanbul

1.2.2 Tsunami History in Marmara

Citizens of İstanbul have not yet been aware of the importance of tsunamis, because rather than any other natural hazard event, earthquake is the most serious natural hazard in the agenda of disaster management strategies in Turkey. However, the historical reports indicating occurrence of tsunamis should also be taken into account in the risk assessment of hazards.

There are scientific studies to investigate tsunami hazard and risk in the Sea of Marmara. Some of the pioneering studies are Yalciner et al., 2002; Altınok et al., 2003; Altınok et al., 2006. The microzonation project granted by İstanbul Metropolitan Municipality have also covered Simulation and Vulnerability Analysis of Tsunamis Affecting the İstanbul Coasts (IMM - OYO Report, 2008).

According to the researches, the maximum height of the tsunami run-up in coastal areas in İstanbul has been noticed as 6 m in 1509 and inundation was shown in some coastal area. The 1894 earthquake takes the second place with about 4.5 m run-up height among the highest tsunamis (Altınok et al., 2011).

The available tsunami catalogs have been compiled and combined in Altınok et al., (2011). Based on GITEC Catalogue criteria, tsunamis having affected coasts of Turkey were presented with the dates and influences in the catalog prepared by Altınok et al., (2011). By considering the reliability of the events, some of the historical tsunamis occurred in the Sea of Marmara and their effects on lands are summarized in Table 1, where TII (Sieberg-Ambraseys Scale; Ambraseys, 1962) is devoted to tsunami intensity. Based on GITEC Catalogue criteria the reliability of source changes in the range of 0-4 where 0: very improbable, 1: improbable, 2: questionable, 3: probable and 4: definite tsunami (Altınok et al., 2011) It is seen from the table that there are 35 tsunami events reported in the Sea of Marmara since 123 AD.; among those 18 tsunami events are noticed as define tsunamis.

Table 1: List of the tsunamigenic event sources in the Sea of Marmara with dates, locations, earthquake magnitudes, tsunami intensities and reliabilities of the events (modified from Altınok et al., 2011)

Number	Year	Source Coordinates	Earthquake Magnitude	TI1	Source Reliability
1	123	40.7N 29.1E	7.2	2	3
2	358	40.75N 29.96E	7.4	-	4
3	368	40.4N 29.7E	6.4	-	1 - 2
4	407	-	6.6	3-4	2
5	447	40.7N 28.2E	7.2	4	4
6	478	40.8N 29E	7.3	-	4
7	488	40.8N 29.6E	-	-	1
8	542	-	6.8-6.5	4	1
9	543	40.35N 27.8E	6.6	4	3
10	549	-	-	-	2 - 3
11	553	40.75N 29.1E	7.0	-	4
12	555	-	-	-	1
13	557	40.9N 28.8E	7.0	4	4
14	740	40.7N 28.7E	7.1	3	4
15	989	40.8N 28.7E	7.2	-	4
16	1039	41.02N 28.5E	-	4	1
17	1064	40.8N 27.4E	7.4	-	1
18	1265	40.7N 27.4E	6.6	-	4
19	1332	40.9N 28.9E	6.8	3	3
20	1343	40.9N 28E	7.0	4	4
21	1419	40.9N 28.9E	6.6	-	2
22	1509	40.75N 29E	7.2	3	4
23	1577	-	-	-	1
24	1648	-	6.4	3	4
25	1751	-	-	-	1 - 2
26	1754	40.8N 29.2E	6.8	-	2 - 3
27	1766	40.8N 29E	7.1	2	4
28	1829	-	7.3	2	1
29	1857	-	-	-	1
30	1878	40.7N 30.2E	5.9	3	4
31	1894	40.6N 28.7E	7.3	3	4
32	1912	40.75N 27.2E	7.3	3-4	4
33	1935	40.64N 27.51E	6.4	2-3	4
34	1963	40.64N 29.13E	6.3	-	4
35	1999	40.73N 29.88E	7.4	3	4

In 358, a tsunami triggered by an earthquake affected İzmit (Yalciner et al., 2002; Altınok et al., 2011). The 553 earthquake was occurred in İstanbul and İzmit Bay (Soysal et al., 1981; Soysal, 1985; Yalciner et al., 2002; Altınok et al., 2011) and the tsunami inundation reached 2000 m on land (Soysal (1985). In 557, a tsunami observed in İstanbul and İzmit Bay (Soysal, 1985) and the tsunami inundation recorded as 3000 m inland (Soysal, 1985; Yalciner et al., 2002). It was noticed that Küçükçekmece region was the most affected region; even religious facilities have been destroyed. Another earthquake-originated tsunami was occurred in 740. Sea water depressions have been observed along the coast of İstanbul, İzmit, İznik and Thrace (Ambraseys and Finkel, 1991; Yalciner et al., 2002). The 989 earthquake

occurred in the eastern part of Marmara and the impact of the tsunami generated by the earthquake was along İstanbul coasts and Gulf of İzmit (Soysal, 1985; Ambraseys and Finkel, 1991; Yalciner et al. 2002; Altınok et al.2011). In 1039, the affected areas by the tsunami were noticed as mainly İstanbul and other coastal region of the Sea of Marmara. It has been recorded that İznik, Bandırma, Mürefte and İstanbul coast have been influenced by a tsunami in 1064. In 1265, tsunami inundation was observed in Marmara Island. The city walls of İstanbul were damaged in 1343 by the effect of the storm rather than a tsunami impact. The waves of tsunami generated by an earthquake in 1419 unexpectedly hit the coasts of İstanbul (Altınok et al., 2011).

One of the most powerful tsunami affecting the Sea of Marmara especially İstanbul was in 1509 (Yalciner et al., 2002). Tsunami waves in İzmit go through the İzmit shipyard, whereas tsunami waves in İstanbul reached to the top of the walls of Galata and inundated the Yenikapı and Aksaray regions. Inundation distance has been predicted about 500-600 meters along the Bayrampaşa stream valley. In 1577, tsunami waves hit the İstanbul coasts. Similar events in the coasts of İstanbul occurred in 1648 and tsunami waves devastated a number of ships around. The 1751 earthquake caused the abnormal waves which dragged few amount of house away (Altınok et al., 2011). A tsunami was generated by an intensive earthquake in 1754 and it affected İzmit Bay (Ambraseys and Finkel, 1991; Yalciner et al., 2002) and İstanbul (Altınok et al., 2011). In 1766, the Bosphorus and the Gulf of Mudanya were damaged respectably by a tsunami caused by an earthquake (Shebalin et al., 1974; Soysal et al., 1981; Papadopoulos and Chalkis, 1984; Soysal, 1985; Yalciner et al.,2002). In the years of 1829, 1857 and 1878, tsunami waves were propagated along the İstanbul coasts, in Kuruçeşme and Bosphorus regions, and in İstanbul, Bursa and Sapanca areas respectively (Altınok et al., 2011).

A strong tsunami triggered by an earthquake was affected İstanbul in 1894 (Ambraseys, 1962; Antonopoulos, 1978; Soysal et al., 1981; Papadopoulos and Chalkis, 1984; Kuran and Yalciner, 1993; Öztin, 1994; Akkargan and Alpar, 2000; Yalciner et al., 2002). The tsunami waves were propagated and inundated 200 m

inland of İstanbul (Yalciner et al., 2002), starting from the region of Büyükçekmece to Kartal districts (Altınok et al., 2011). The run-up height of tsunami was less than 6 m and earthquake magnitude was less than 7.0 (Öztin and Bayülke, 1991; Yalciner et al., 2002). The Karaköy and Azapkapı bridges were inundated (Batur, 1994). The run-up height was recorded as 1.5 m in Yeşilköy and 4.5 m at the Azapkapı Bridge (Altınok et al., 2011). In 1912, Şarköy-Mürefte Earthquake is known as one of the destructive earthquake caused a tsunami. The affected regions were Şarköy, Mürefte, İstanbul and Ganos (Altınok et al., 2011). Fishery boats nearby Yeşilköy in İstanbul were rose up 2.7 m with the increase of sea level (Yalciner et al., 2002; Altınok et al., 2011). The 1935 earthquake resulted in the devastation of the villages of Marmara Island (Yalciner et al., 2002; Altınok et al., 2011). The effect of the earthquake was felt in also Tekirdağ, Edirne, İzmir and Bursa cities (Altınok et al., 2011). Another destructive earthquake triggering a tsunami was in Yalova and Çınarcık in 1963; the epicenter of this earthquake was in the sea. The height of waves reached 1 m in Bandırma (Özçiçek, 1996; Yalciner et al., 2002; Altınok et al., 2011).

The last disruptive and fatal earthquake with a magnitude of 7.4, known also as İzmit Bay tsunami, occurred in the Gulf of İzmit in 17 August 1999 and resulted in the loss of 18850 people (Alpar, 1999; Alpar and Yaltırak, 2000b; Altınok et al., 2011). Its effect was spread on a large area, and its surface rupture was mapped at least 50 km in offshore with 5 m right lateral offset and 3m vertical offset. The main fault moves towards the center of the depressions in the bay. The secondary faults which are the oblique components by low angle to the main fault were created by the dextral shearing mechanism (Altınok et al., 1999; Şengör et al., 1999; Alpar and Yaltırak, 2000a, b; Yalciner et al., 2002). Depending on the movement of tsunami waves, uniform recessions have been observed along northern to southern shorelines, starting from the central sub-basin of İzmit Bay to the east of Hersek Delta (Altınok et al., 1999, 2001b; Yalciner et al 2002). Tsunami period was measured as less than a minute. The characteristic of the master fault has been determined as strike slip fault. Besides the tectonic movements, marine landslide near Değirmendere was one of the reasons of tsunami waves (Yalciner et al., 1999, 2000; Yalciner et al., 2002). The maximum run-up height was measured as 2.66 m along the region between

Tütüncüçiftlik and Hereke, while 2.9 m in Değirmendere and 3 m along the coast from Değirmendere to Karamürsel (Altınok et al., 2001b; Yalciner et al., 2002). The maximum inundation was observed more than 300 m at Kavaklı (Altınok et al., 2011).

1.2.3 Geology of the Study Area

With respect to the distribution of rocks on land, the basement of the Sea of Marmara is predicted as Paleogene sedimentary rocks. The age of rocks exposed at the northern and southern portions are Eocene or Oligocene, and Paleocene, respectively. The bottom shelf follows the depression from onshore to the offshore approximately 100 m with gentle angles. Shelf and basin consists of unconsolidated silt and clay above the basement. The maximum depth is measured as 1300 m from the sea level to the sea bottom (Dalgıç et al., 2009).

The geological structure of İstanbul region is complex because of the repeating nature of similar deposits, unclearness of reference layers, the presence of orogenic activities, interference folds, and a great number of andesite and diabase dykes. The European basement of İstanbul consists of Carboniferous, Eocene, Oligocene, Miocene and Quaternary sedimentary rocks and thick filling material in closer areas to the shoreline (Figure 3). Dykes in the geological structures cause problems because of their decomposition and discontinuous characteristics. Karstic cavities in Eocene Kırıkkale formation, landslides in the clayey-silty lensed strata of the Oligocene Gürpınar formation, swollen soil caused by earthquake in clayey-silty lensed strata of Miocene Güngören formation, Quaternary alluvium, and insufficient bearing capacity of thick filling material are the problematic characteristics of the European portion of İstanbul (Dalgıç et al., 2009).

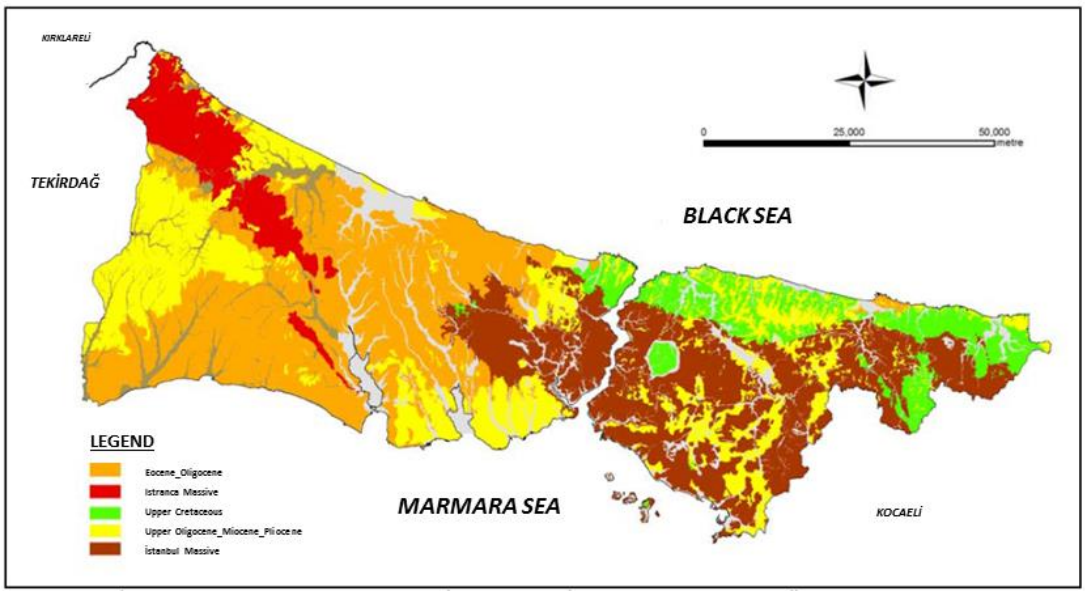

Figure 3: The geological map of Istranca and İstanbul region (modified from Özgül, 2011)

In the European side of İstanbul, the dominant rock units are Carboniferous Trakya Formation, consisting of sandstone, siltstone and limestone, and cross-cutting andesite and diabase dykes. Eocene, Oligocene and Miocene deposits overlie Trakya Formation. Trakya Formation was exposed to intense deformation expressed by folds, fault and joints. The thickness of the formation is predicted as more than 1000 m. Trakya formation is overlain by Eocene Kırklareli Formation with a thickness of 150 m. This Eocene formation consists of partly thick-bedded, micritic, porous and fossiliferous limestone, marns and calcareous claystones. The sequence continues with Oligocene Gürpınar Formation more than 700 m. Gürpınar Formation is made up of sandstones and clay-claystone alternations. Çukurçeşme Formation, which is the oldest formation of the Miocene sequence, overlies Gürpınar Formation with a thickness of the 25 m and it comprises partly unconsolidated conglomeratic sand and clay layers or lenses. Güngören Formation overlies Çukurçeşme Formation. The formation is composed of greenish gray, light brown colored clay layers including fine sand lenses. The youngest unit Miocene unit is Bakırköy Formation with a thickness of 20 m. It is composed of by white colored, greenish gray clay marn and limestone. The alluvial deposits consist of yellow, brown colored sand and silty clay,

but also fiord deposits made up of silty clays with 35m depth. At the upper most layers, the sequence is completed with the deposits of antique and current filling materials, about 30m thick (Dalgıç et al., 2009). The generalized stratigraphic columnar section is presented in Figure 4.

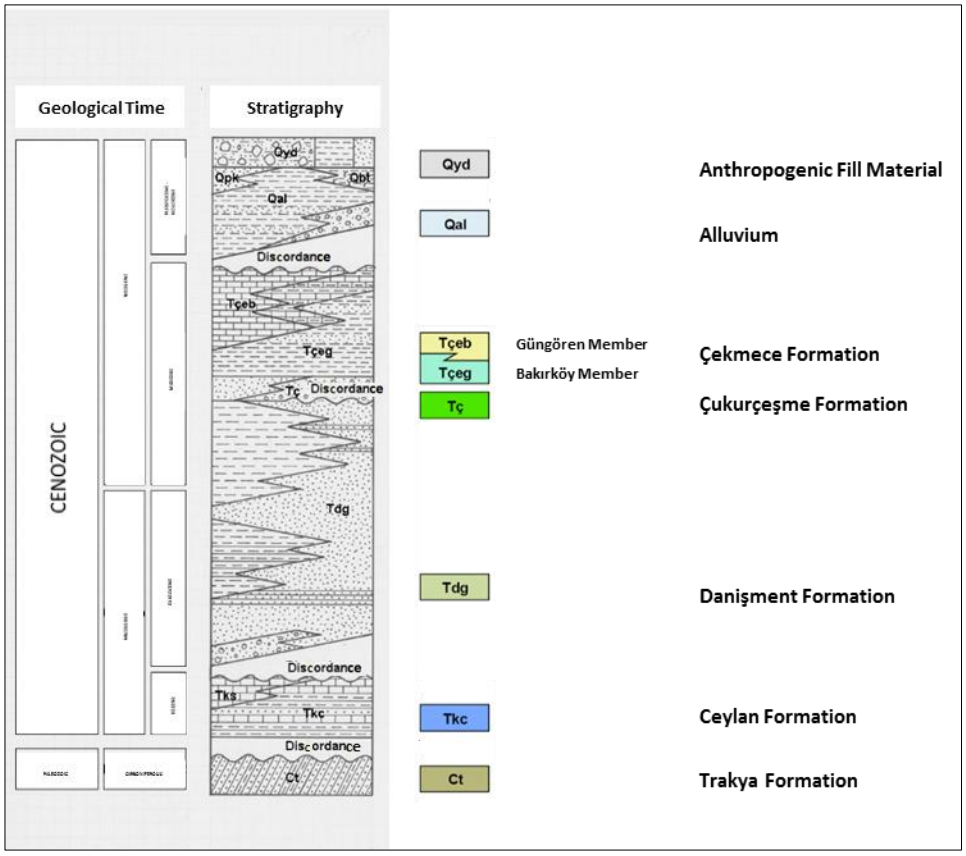

Figure 4: Generalized stratigraphic section of the study area (modified from URL-1 and IMM, 2015)

1.2.4 Seismicity of Marmara

The Anatolian Peninsula lies in the Mediterranean region of Alpine-Himalayan orogenic belt and it is controlled by three main faults and a subduction zone (Bozkurt, 2001): (i) North Anatolian Fault (NAF) zone, (ii) the East Anatolian Fault zone, and (iii) Dead Sea Fault zone and (iv) the Hellenic arc (Figure 5). Although general structure of NAF is right lateral strike slip fault, it also has normal components at some locations: south of Prince's Island, north of Marmara Island and

Yalova. The dextral NAF divided into 3 branches around 31 °E longitude. The northern branch follows the Sea of Marmara to the Gulf of Saros and it enters to the North Aegean Through, whereas the southern branch extends to Yenişehir (Bursa) to the south on the land. The middle branch continues the Marmara coastline from Gemlik Bay to Bandırma and connects into the Aegean Sea (Mercier et al., 1989; Kuran and Yalciner, 1993; Yalciner et al., 2002).

The Anatolian Block is being extruded westward within the ongoing neotectonic regime at a rate of about 24 mm/yr on the northern branch of transform NAF (Straub and Kahle, 1997), and brings increasing stress accumulation along the Sea of Marmara region (Yalciner et al., 2002). Marmara is one of the seismically active zones of the world because of this unstable tectonic system and many large-scaled earthquakes occur at Marmara region with mostly strike slip mechanism. With the August 17, 1999, Kocaeli earthquake on the northern branch of NAF has increased the earthquake risk in the Sea of Marmara (Parsons et al., 2000). According to the past records, more than 300 earthquakes are reported in the Sea of Marmara. (Soysal et al., 1981), showing high earthquake activity. Likewise earthquakes, many researchers are reported that 90 major tsunami events occurred in the Turkish coasts in the past 3000 years and the most of them was in the Sea of Marmara (Altinok and Ersoy, 2000).

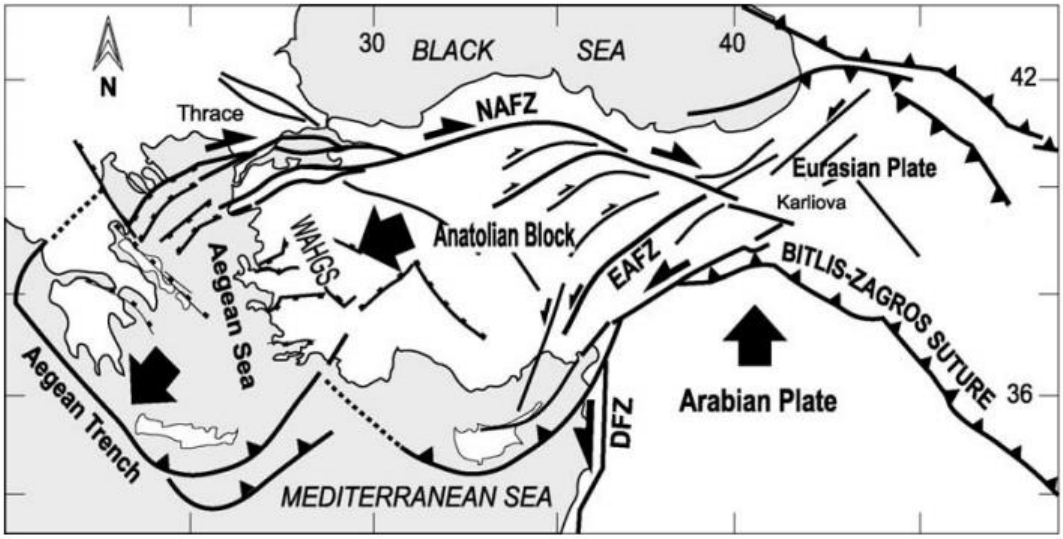

Figure 5: Tectonic outline of Turkey. DFZ: Dead sea Fault Zone, EAFZ: East Anatolian Fault Zone, NAFZ: North Anatolian Fault (Gürer et al., 2002).

1.3 Literature Survey on Geographical Information System (GIS) based Tsunami Vulnerability Assessments (TVA)

Tsunami is one of the most important marine hazards generally generated by earthquakes and/or submarine/subaerial landslides. Tsunami may be very effective along very large regions mostly far away from the generation region.

Risk assessment is related to the results of the hazard and the vulnerability assessments. In the hazard assessment the main point is to find out hazardous zones and related probability of tsunami hit to land.

There are many places all over the world which are very vulnerable to the impacts of tsunamis and exposure along the coasts. This is why majority of scientists have been focused on the tsunami assessment to estimate the structural damage and fatalities because of tsunami events and to contribute to the development of the tsunami risk alarm system.

A pioneering study is conducted by Papathoma et al., (2003), and a new tsunami vulnerability analysis model was proposed namely, Papathoma Tsunami Vulnerability Assessment Model (PTVAM). In this study, the proposed model offers a GIS-based method of estimating the vulnerability of buildings to a potential tsunami treat. According to the researches, the reliability of the collected data including historical tsunami events is essential to prepare an accurate tsunami model. For this reason, related reports and records were evaluated very carefully by considering their reliability and accuracy. These reports were also a starting point of the tsunami vulnerability assessment (TVA). The collected data from the historical tsunami events, tsunami propagation and its inundation were modeled. Physical parameters of the inundation (e.g. inundation distance, flow depth, run-up height and current) were determined by considering the results of model. The probabilities or return periods of the tsunami events are analyzed and the results are provided as thematic maps and GIS layers for the national and regional planning institutions.

Since preparation of a well-supported model which can help to identify fragility of buildings located within tsunami inundation zone is hard, Papathoma Tsunami

Vulnerability Assessment (PTVA) has been developed to estimate vulnerability of buildings. The main steps of the PTVA model are 1) collecting hazard data to determine tsunami scenario and geo-spatial data to develop tsunami hazard model and collect geo-spatial data in hazard zone; 2) calculating vulnerability numerically and developing GIS-based maps such as vulnerability, probable maximum loss, etc.; 3) mapping and recommendations to end users such as emergency services, insurance companies etc. This model has been validated by applying many studies in last decade, since it was proposed in 2003 by Papathoma and Dominey-Howes. Then, it was revised in 2007 by the same authors and revisions has been continued with Dominey-Howes and Papathoma, (2007), Dall'Osso et al., (2009b) and Dominey-Howes et al. (2010). Three different forms of PTVA models have been published: namely, PTVA-1 - Herakleio, Crete, Greece (Papathoma et al., 2003) and the Gulf of Corinth, and Greece (Papathoma & Dominey-Howes, 2003); PTVA-2 – Seaside, Oregon, USA (Dominey- Howes et al., 2010); PTVA-3 – Sydney, Australia (Dall'Osso et al., 2009a) and the Aeolian Islands, Italy (Dall'Osso et al., 2010)

Papathoma et al., (2003) also focused on describing the frequency and magnitude of tsunami events and producing inundation maps which help to forecast vulnerability of uniform population, infrastructure, business; she gave a new insight to tsunami hazard studies by determining and developing new methods consisting of natural and built environments parameter in the example from Herakleio, Crete (2002). Their way contributing to tsunami vulnerability assessment has been applied on Greek coasts, particularly in Herakleio, Crete. The results obtained by their model have been presented as thematic maps by Geographical Information System (GIS).

In 2003, Papathoma & Dominey-Howes carried out a new tsunami vulnerability model by assuming 7th February 1963 tsunami as a worst case scenario. This study was applied to two village located in the coastal region, in the Gulf of Corinth, Greece since it is known as one of the most seismically active places in the world. Recent studies have showed that vulnerability of buildings is very important as much as other dynamic components based on a number of parameters (Papathoma and Dominey-Howes, 2003). The areas in the two coastal villages, Akoli and Selianitika,

have been classified depending on the vulnerability of buildings located in by considering their type and the population within. Since the run-up cannot be calculated, the highest record tsunami wave recorded between the coastline and the maximum inundation line on lands, 5m, was used for the determination of the tsunami vulnerability of the structures. The results have been presented very carefully in order to use in disaster management planning in the coastal risk areas.

Tarbotton et. al., 2012 has been determined a geographical information system (GIS) based method called Papathoma Tsunami Vulnerability Assessment (PTVA) in order to forecast vulnerability of buildings to potential tsunami disaster. In the lack of recognized fragility functions/curves of buildings enough, PTVA give better results to determine vulnerability of buildings and populations and guessing extent of damage by a tsunami.

Omira et al., (2010), conducted a study of tsunami vulnerability assessment in Casablanca-Morocco by combination of tsunami numerical modeling, field survey data and GIS tools. They have been computed inundation boundary, inundation flow depth and vulnerability of building stock in the Casablanca Harbor and its surroundings. They divided the study in two steps as i) hydrodynamic modeling and inundation mapping, and ii) development of a new vulnerability estimation model by evaluating vulnerability of building of large areas and type of building structures. It is stated that in order to develop a new model for TVA, researchers collected data from the study area and combined them with the hydrodynamic modeling. GIS tools were provided them to generate the vulnerability maps.

More specifically, the Lisbon event has been chosen as the worst case scenario resulted in with tsunami impact for tsunami modeling. Cornell Multigrid Coupled Tsunami Model by Cornell University has been used and the simulations have been prepared along the largest tsunamigenic area in the North Atlantic which is covering the eastern domain of the Azores-Gibraltar fracture zone. To define the vulnerability of the buildings, authors visited the coastal area of Casablanca and determined the building types located in the study area. It is found that besides in dynamic concepts, irregular distribution of vulnerability in flood zone, depends on various parameters.

Researchers have been developed an upgradable database which allows producing new vulnerability maps. They estimated a model for vulnerability assessment on building stock, namely Building Tsunami Vulnerability (BTV). The worst case scenario has been used to display vulnerability maps derived by the developed model by GIS tools.

Koshimura et. al., (2009), focused on the tsunami fragility on the structures in the region damaged by tsunami waves. Shuto's Intensity Scale (1993) has been used to discuss the structural damage on land. They developed the fragility functions (fragility curves) as a new measure for estimating the damage on structures and environments. These fragility functions have been related with the performing seismic risk analysis of structures and identification of the structural vulnerability when strong earthquakes or landslides occur. These curves also were developed by integration of numerical modeling of inundation on the land and GIS analysis of historical tsunami survey data of the 2004 Sumatra-Andaman earthquake tsunami disaster in Banda Aceh, Indonesia. This study was mainly about expressing the fragility functions depending on structural probable damage or human loss in the region by considering hydrodynamic features of tsunami inundation flow (inundation depth, current velocity and hydrodynamic force). It is found that the capability of forecasting potential tsunami events and their damage by using fragility measurement. By this way a bridge has been created between local vulnerability and tsunami hazard by numerical modeling relationship.

Santos et al., (2014), carried out a study and brought out a new approach for tsunami vulnerability assessment. It is based on a comparison of two different models applied on the same area, Setubal city in Portugal. By collecting the data from the past tsunami records, a tsunami source having the same characteristic with 1755 Lisbon Tsunami has been simulated so as to use in the comparison of tsunami vulnerability assessment (TVA) models, namely PTVA-3 (2009) and Model B. Different from the PTVA-3 model, Model B involves Structural Vulnerability Index (SVI) developed by Ismail et al. 2012 and it also excludes the parameters referring to protection level. Since PTVA-3 method focused on Vulnerability of buildings, as the previous studies,

the influenced buildings were classified with the help of validated, 10m-resolution orthophotography. Authors used GIS-based MCDA to compute the SVI including set of parameters. Collection of data, visualization of the results, and validation of decision making processed have been conducted by GIS tools.

1.4 Data and Methodology

1.4.1 Available Datasets

There are two available datasets. The topographical dataset is obtained from the Directorate of Cartography underneath of Department of Housing and Urban Development of İstanbul Metropolitan Municipality (IMM) and the bathymetry dataset is derived from Nautical Charts of Navigation, Oceanography and Hydrography Department from Turkish Navy. The IMM data are digital elevation model (DEM) covering the entire İstanbul region with 5m spatial resolution and the vector data includes all structures and infrastructures in the Fatih district of İstanbul. These two available dataset are explained in detail in Section 3.3.

1.4.2 Methodology

The methodology of the whole study will be presented step by step in the next chapter; thus a glimpse of the study methodology is disclosed in this part. The brief ordered list of steps applied through the thesis is as follows:

1. Tsunami Numerical Modelling (TNM),
2. GIS-based vulnerability assessment mapping and Mapping by using Multicriteria Decision Making Analysis (MCDA) Model, Analytical Hierarchy Model (AHP)
3. The interaction of the former two resulting in GIS-based Tsunami Hazard Assessment

a) Tsunami Numerical Modeling

For Tsunami Numerical Modelling, the available topographical and bayhymetric datasets are used as input data for tsunami simulation software to calculate the inundation and the run-up onto the near shore and to observe the probable damage inland. A database was created by bathymetry, topography and shoreline data of the Yenikapı and used for high resolution tsunami numerical modelling by NAMI DANCE to calculate necessary tsunami parameters of tsunami behavior in shallow water and in inundation zone.

b) Tsunami Risk Assessment (MCDA with GIS)

For GIS-based vulnerability assessment, metropolitan use and topographical data from IMM is manipulated and various thematic maps were produced not only for vulnerability but also for the evacuation easiness of the area. GIS-based Tsunami hazard assessment in the region is performed by a MCDA model. AHP framework is constructed and locational vulnerability with evacuation resilience maps are prepared.

c) Tsunami Hazard Assessment

The depth of tsunami waves the scores of locational vulnerability and evacuation resilience is used to propose an equation to generate the tsunami hazard map in GIS environment.

CHAPTER 2

TSUNAMI SIMULATIONS

Tsunamis are determined as a series of the giant waves generated by mostly submarine earthquakes, undersea landslides, volcanic eruptions and impacts of objects from outer space (such as meteorites, asteroids, etc.). As a known fact tsunami waves dramatically increase in height in the depths of the ocean, furthermore their height become higher and higher as the waves reach the inland while the depth of the ocean is decreasing. The abrupt displacement of the water makes the power of tsunamis be extremely high. The tsunami waves are extremely long length and effective in long period. These waves cannot be compared with the waves generated by winds, since the period, wavelength and velocities of the tsunami waves are mostly a hundred times larger than the wind-caused waves. There are six stages of tsunami motion which is called “life of a tsunami” by USGS, 2015 as (i) initiation of the wave due to generation mechanism, (ii) split, (iii) propagation, (iv) near shore amplification, (v) run-up and impact and (vi) inundation.

(i) Initiation of the wave due to generation mechanism: Tsunamis are initiated by a sudden displacement of the ocean, commonly caused by vertical deformation of the ocean floor during earthquakes. The seafloor is "permanently" uplifted and down-dropped, pushing the entire water column up and down because of the submarine earthquakes. An abrupt deformation occurs in the sea floor and the overlying water is displaced from its equilibrium position. The reaction time is not very long in region close to the earthquake epicenter caused the tsunami. Other causes such as submarine landslides, which often occur during a large earthquake, can also generate tsunamis. During a submarine landslide, the equilibrium sea-level is changed by sediment moving along the sea-floor. Then the propagation of the tsunami by gravitational

forces causes the initial perturbation of the sea level. Volcanic eruptions can also cause a displacement of water and generate a tsunami.

The mechanisms which cause tsunami generate potential energy and it turns to the kinetic energy which is horizontal propagation of the tsunami wave. In deep water tsunamis are not large and pose no danger. They are very broad with horizontal wavelengths of hundreds of kilometers and surface heights much smaller, about one meter. However, as the wave approaches the shore and the water shallows, all the energy that was distributed throughout the ocean depth becomes concentrated in the shallow water and the wave height increases.

ii) Split: In a short span of time after the earthquake, the initial tsunami is split into two oppositely traveling tsunamis which are above mean sea level and are approximately half of the original tsunami. One of the split part of tsunami travels out to the deep ocean (distant tsunami), whereas another approaches towards the nearby coast (local tsunami). Since the speed of the both tsunami diverse as the square root of the water depth, the distant tsunami travels faster than the local tsunami.

iii) Propagation: Long waves propagate with very low energy loss and their range reaches at all coasts of the basin. Its propagation speed is directly related the square root of gravitational acceleration and water depth as given in the following relation (Equation 2.1.).

$$C = sqrt\ (g * d) \tag{2.1}$$

Where C is the speed of tsunami propagation, d is water depth and g is gravitational acceleration. It is clearly seen from the relation that tsunami propagation speed is faster in deep sea.

iv) Near shore amplification: The distant tsunami will reach the coastal areas at far distances and slows down when water depth decreases. The only energy loss is bottom friction and it is very small. At shallower regions the rule of conservation of mass causes tsunami with higher amplitude and strong currents. However the

reflection is also another phenomenon -which cause amplification in semi enclosed basins.

v) Run-up and impact: When the tsunami moves inland from the deep water, the water level can rise up to many meters with strong currents whose momentum cause propagation of wave into land area as inundation. The vertical distance between the point of inundation front and the reference level (e.g. still water level – SWL or mean water level MWL) is determines as run-up.

Tsunami waves are very powerful and extremely rapid waves while comparing the normal waves (wind-generated waves. etc.). Run-ups are the most damaging force inland, since tsunamis are caused by strong currents which also carry floating debris. Thus, it is unavoidable for the most of the buildings and/or structures onshore to be damaged. The topography of the shoreline is a factor affects the height of run-up onshore. The larger waves occur where there are steep walls or cliffs.

vi) Inundation: Main impact of tsunami occurs at shallow regions (generally at near shore) and coastal areas. It is inundation and several tsunami parameters can be defined at inundation zone.

Tsunami hazard assessment need to determine potential risky zones by metrics which include tsunami impact and reflect distribution of tsunami forces over the whole affected area. Maximum and minimum wave elevation, maximum flow depth and maximum current speed are determined in metric form to determine the tsunami damage on the shoreline (Figure 6).

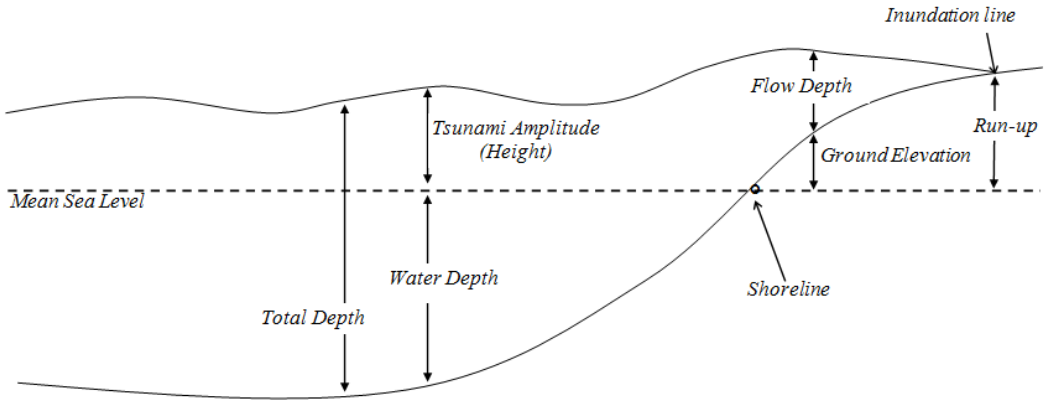

Figure 6: Schematic representation and basic definitions of tsunami parameters for near shore (modified from URL-2)

Tsunami numerical modeling is one of the essential tools to describe the possible tsunami scenarios and their impacts as mathematical description. Modeling starts with the potential worst case scenarios for the tsunami sources or for the run-up and inundation generated by a local or distant tsunami, since they are more reliable than the past tsunamis. Modeling provides what to analyze the potential tsunami strength and the impact on the shoreline by the help Geographical Information System (GIS) for preparing bathymetry and topography data. It is stated in Tsunami Risk And Strategies For the European Region (Yalciner et al., 2005) that tsunami modeling has several phases which can be summarized as (i) catalogue and literature survey on the historical tsunamis, (ii) determination/development of bathymetry/topography data, (iii) determination of current land use plans in GIS based format, (iv) determination and characterization of probable tsunami sources, (v) computing the tsunami source characteristics from using estimated rupture characteristics and landslide characteristics, (vi) determination of study domains for modelling, (vii) simulation and computing all necessary tsunami parameters, (viii) inundation mapping, (ix) probabilistic analysis (x) dissemination of results, (xi) animations and 3D visualizations of selected tsunami scenarios and (xii) providing data and specific information to authorities for developing guidelines and mitigation measures in accordance with the land use plans.

Active faults are the most efficient triggers for the generation of tsunamis. If the tsunami sources (such as active faults, landslides etc.) are indicated with the mechanism and the nature (such as type, location and scale) is explained with the information of the past historical tsunamis, such determined scenarios are called "Tsunami Scenarios". For tsunami hazard assessment, the tsunami parameters are calculated using the information about selected tsunami sources in tsunami simulations. Appropriate bathymetry and topography data are inputted into tsunami numerical model. The coordinates and elevations of the existing structures/buildings (such as houses, bridges, etc.) are combined with the correct ground elevation in appropriate coordinate systems by the help of GIS-based softwares.

Tsunami hazard assessment needs expertize from basic, applied, and administrative sciences. There was only little number of studies on tsunami hazard assessments in Turkey until the 1999 Kocaeli earthquake. 2004 Indian Ocean tsunami is drawn strong interest of researchers and targeted research directions to tsunami hazard assessment not only at scientific but also in operational level.

Many tsunami events have occurred in the Mediterranean Sea, the Black Sea, the Sea of Marmara, and the Aegean Sea, which may warn that there would be another tsunami in the region. Before disasters come across, the possible effects of tsunamis should be forecasted and disaster mitigation measurements should be developed accordingly. Additionally, the required tsunami hazard assessments should be performed.

The distribution of structure and/or buildings, variation of the building type and their vulnerabilities are one of the key elements to understand the level of tsunami hazard in a given area. Tsunami hazard map is another useful product of modeling for visualizing the spatial distribution of tsunami risk.

This study is focused on tsunami parameters obtained by numerical modeling, and, locational vulnerability and evacuation resilience analyses with GIS support.

2.1 Tsunami Numerical Modeling

Tsunamis are natural hazards which may cause loss of life and property damage when they hit shores. However, preparations for emergency plans take an importance role to decrease the damage in these cases (Ayca, 2012). Obviously, with advanced computation technology, numerical modeling studies will help to obtain more realistic results.

Increasing awareness to tsunami hazard and decreasing disaster mitigation for tsunamis need close collaboration of scientists and professionals at international level. Mitigation of tsunami impact can be achieved by providing faster evacuation for human and by increasing resistivity and performance of structures against tsunamis.

Tsunami modeling is one of the important phases of tsunami hazard assessment. The source mechanisms, bathymetric and topographical data in adequate resolution, selection of probable tsunami scenarios are used in tsunami numerical modeling.

Heidarzadeh et al., (2008), conducted a study to examine the tsunami effect in Makran Subduction Zone (MSZ), along the coasts of Iran and Pakistan, by numerical modeling of past tsunami in the area. Although MSZ is known for generating the second critical scenario among all tsunami amongst the study area, the results are rough. The five critical scenarios based on past records were also examined, and then the simulations were undertaken by numerical modeling. This study helped to assess the 1945 Makran tsunami in detail and to clarify uncertainties in the past records by numerical modeling. It also helped to simulate tsunami generation and to calculate run-up heights in selected coasts by the source of MSZ. Regarding the results of the numerical modeling, the records would be overrated, although historical records stated that 12-15 m run-up heights were observed in the region in 1945 Makran tsunami. It is concluded that if the past records are reliable, the reason of large run-up heights would be either enormous submarine landslides by an earthquake or the huge displacement in the rapture.

Özer and Yalciner, (2011), studied sensitivity of hydrodynamic parameters during

numerical simulations of tsunami inundation. In this scenario, two basins with different bottom slopes, considering some of major tsunami parameters such as maximum positive amplitudes, flow depths and maximum currents respectively, were simulated by using numerical model, TUNAMI-N2 (prepared by Tohoku University). The parameters for different slopes were compared. Hence, high resolution data is recommended for the future studies in order to obtain more accurate results at bottom condition. The necessary hydrodynamic parameters for this study were computed by numerical modeling.

Kaiser et al., (2011) utilized tsunami numerical modeling in order to obtain inundation parameter to examine the effect of land cover roughness. The main approach of this study is to generate spatial and temporary information on inundation characteristics by focusing on land cover roughness. In this way, it is aimed to contribute to the studies of damage analysis and risk assessment related to the 2004 Indian Ocean tsunami. The influence of two main factors, vegetation and build environment, on tsunami inundation have been investigated by numerical modeling related to the 2004 Indian Ocean tsunami. The case study has been performed in the coastal provinces of Thailand's most affected areas. Bathymetry, topography, bottom roughness and wave expressions of tsunami source have been generated and land cover classification has been done by high resolution satellite imagery. Tsunami inundation maps are prepared. The influence of land cover roughness is observed. Moreover, the effects of build environment were examined for both rural and urban areas. By considering the results of the numerical modeling and the presented inundation maps, it is concluded that inundation parameters such as flow depth and flow velocity on land are affected by the land cover and/or build environment; moreover topography is the most critical factor that affects the inundation parameters.

Another study about numerical modeling was carried out by Ayca, (2012). It is intended to provide a Web-based application serving tsunami inundation maps by using GIS. The Sea of Marmara (Turkey) was selected for this study. By following deterministic approach, several tsunami scenarios have been performed for the

affected region. The generation of the scenarios was based on OYO-IMM Report (2008), but the displacement of faults has been exaggerated 2 times. Inundation parameters such as run-up heights and flow depth have been calculated and tsunami inundation maps have been presented by GIS tools. The results have been validated for the region of Sea of Marmara to serve through internet after completing the process of the generation of web interfaces. The study was concluded by comparing the effects of the critical scenarios for each affected region were presented and the derived results by numerical modeling were discussed. Additionally, capabilities of the internet based application have been examined.

2.1.1 Tsunami Computational Tool for Numerical Modeling

There are several remarkable computational tools which admit direct simulations and efficient visualization of tsunamis for assessments, understanding and prospecting of tsunami generation and propagation mechanism. The most important contribution was made by Shuto and Imamura by creating TUNAMI N2 (1989-1990). TUNAMI N2 was followed by several numerical models such as AVI-NAMI (developed by C++ programming language and developed/distributed under the support of UNESCO), and NAMI DANCE (tool developed by Andrey Zaytsev, Ahmet Yalciner, Anton Chernov, EfimPelinovsky and Andrey Kurkin). These tools are capable to compute near shore and inundation parameters such as maximum positive amplitude, maximum current velocity, flow depth, run-up, inundation distance, discharge flux, momentum flux, hydrodynamic load, maximum negative amplitude (NAMI DANCE, 2013).

Making prediction of possible tsunami hazards and knowing risks by numerical modeling, generating possible tsunami sources provide taking precautions against these disaster or natural calamities (NAMI DANCE, 2013).

NAMI DANCE is one of the most capable computational tools for tsunamis. NAMI DANCE uses bathymetric and topographical data, tsunami source data (from rupture

parameters or any other user defined initial water elevations). It solves non-linear form of equations in single or nested domains.

The initial wave from the different sources can be created by selecting the required source parameters consisting of epicenter coordinates, length of the fault, the width of the fault, strike angle, dip angle, rake, vertical displacement of the fault, focal depth. The generation of the sea state at specific time intervals of tsunami during simulations is also possible. After completing the run-up calculations, it allows 3-D plotting of the sea state at a specific time interval. NAMI DANCE provides efficient visualization and animations of the results in 3-D view after direct simulation. (NAMI DANCE, 2013)

NAMI DANCE is valid and verified numerical code and it has already been applied to different tsunami events for tsunami hazard analysis. Some of those references are (Yalciner et al., 2010; Yalciner et al.,2011, Heidarzadeh et al., 2013; Özer and Yalciner, 2013; Yalciner et al., 2014; Dilmen et al., 2014; Özer et al., 2014).

NAMI DANCE provides the distribution of the tsunami parameters at near shore and inundation zone. Those parameters are important to implement the magnitude of tsunami in vulnerability analysis.

2.2 Selection of Tsunami Source Parameters for the Study Area

Tsunami source is the initial form of the water surface which is generated by sea bottom deformation due to rupture of earthquake and/or submarine landslides. The determination of these mechanisms is one of the most significant phases of tsunami risk assessment. The rupture parameters (epicenter, width and length of the fault plane, dip, rake and strike angles, focal depth and vertical displacement of fault) are necessary for producing tsunami source.

In this study, the critical tsunami scenarios for Yenikapı are selected from different reports and papers considering seismic mechanism (Yalciner et al., 2002, Hebert et

al., 2005, OYO-IMM Report, 2008; Ayca, 2012). There are 6 potential sources which may responsible for generation of tsunami in the Sea of Marmara. They are the Prince's Islands (PI) (oblique-normal) fault, the Prince's Islands (PIN) (normal) fault, Ganos (GA) (oblique-normal and oblique-reverse) fault, Yalova (YAN) fault (oblique-normal and normal), Central Marmara (CMN) (normal) fault and the combination of PI and GA. Among these, the sources PIN and YAN are selected as critical scenarios which may cause tsunami with higher water level, flow depth and stronger current velocities at Yenikapı (Figure 7 and Figure 8). The rupture parameters of each segment that belong to PIN and YAN sources are given in Table 2 and Table 3 (Ayca, 2012; Özdemir, 2014).

Tsunami source PIN is the normal component of the first four oblique-normal segments of tsunami source PI (Table 2). In the simulations, it is assumed that four segments of PIN rupture have been broken entirely and generated the tsunami source with the maximum positive amplitude as +1.05 m and maximum negative amplitude as -2.57 m (Ayca, 2012) (Figure 7).

Tsunami source YAN is consisted of 8 segments in which 3 of them are oblique-normal and 5 of them are normal fault (Table 3). In the simulations, it is assumed that 8 segments of YAN rupture have been broken entirely and generated the tsunami source with the maximum positive amplitude as +1.03m and maximum negative amplitude as -2.51 m (Ayca, 2012) (Figure 8).

Table 2: Estimated rupture parameters and initial wave amplitudes for tsunami source PIN (Ayca, 2012)

Fault	Type	Longitude (ED_50)	Latitude (ED_50)	Depth from sea bottom	Strike	Dip	Rake	Length	Width	Vertical Displacement	Initial Wave Amplitude	
		degree	degree	m, GL-	degree	degree	degree	m	m	m	Max (m)	Min (m)
PIN	Normal	29.12942	40.75691	744	108.15	70	270.00	8753	17027	5.00	+1.05	-2.57
		29.06928	40.78610	740	123.15	70	270.00	6024	17027	5.00	+0.94	-2.41
		28.99465	40.81653	779	118.85	70	270.00	7148	17027	5.00	+0.98	-2.47
		28.90432	40.87251	1210	129.90	70	270.00	9834	17027	5.00	+0.92	-2.36

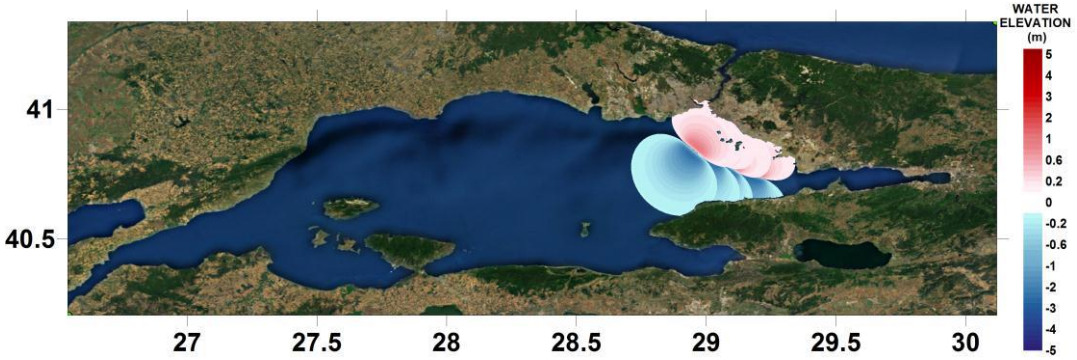

Figure 7: Tsunami source Prince's Islands Normal (PIN) Fault (Ayca, 2012)

Table 3: Estimated rupture parameters and initial wave amplitudes for tsunami source YAN (Ayca, 2012)

Fault	Type	Longitude (ED_50)	Latitude (ED_50)	Depth from sea bottom	Strike	Dip	Rake	Length	Width	Vertical Displacement	Initial Wave Amplitude	
		degree	degree	m, GL-	degree	degree	degree	m	m	m	Max (m)	Min (m)
YAN	Oblique-Normal	29.47103	40.72115	1978	257.96	70	195.00	7058	17027	5.00	+0.49	-1.56
		29.38946	40.70750	1960	261.14	70	195.00	6873	17027	5.00	+0.60	-1.65
		29.30920	40.69751	1823	260.98	70	195.00	10952	17027	5.00	+0.92	-2.35
	Normal	29.18143	40.68121	1681	262.35	70	270.00	4448	17027	5.00	+0.52	-1.55
		29.12936	40.67550	1557	273.96	70	270.00	4562	17027	5.00	+1.03	-2.51
		29.07551	40.67791	1252	283.78	70	270.00	10021	17027	5.00	+0.53	-1.79
		28.96007	40.69843	1219	294.84	70	270.00	3154	17027	5.00	+0.56	-1.77
		28.92602	40.71005	1178	284.90	70	270.00	14043	17027	5.00	+0.78	-2.15

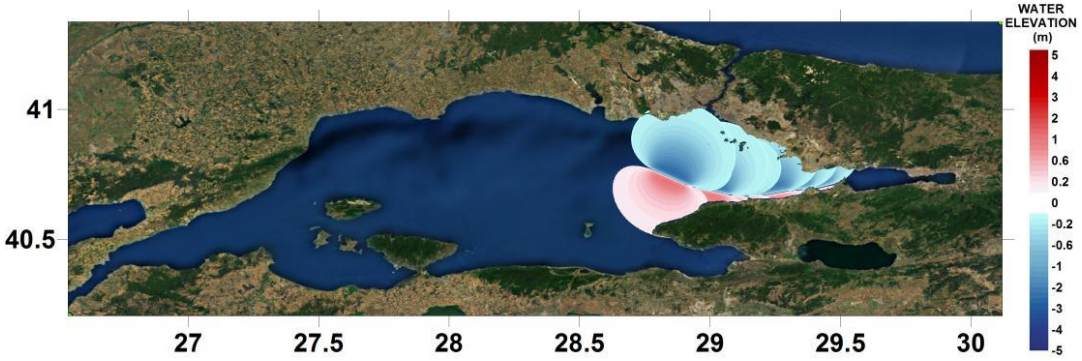

Figure 8: Tsunami source Yalova Normal (YAN) Fault (Ayca, 2012)

Tsunami numerical modeling needs proper determination of the source parameters, development of high resolution topography and bathymetry, and valid/verified computational tools. In the following sections, data processing by GIS implementations to obtain high resolution topography and bathymetry for numerical modeling as well as study domains are presented. Furthermore, the simulations and the simulation results are also presented and discussed.

2.3 Domain Selection for Tsunami Analysis

The nested domains are created as high resolution, covering the Yenikapı region and environs. Three nested domains (from large to small B, C, and D) are selected in different resolution. The corner coordinates and maps of these domains are given in Table 4 and Figure 9, respectively. The largest domain (B) covers the whole Marmara in about 90 m resolution, the medium domain (C) covers Yenikapı region with 30 m resolution, and the smaller domain (D) with 10 m resolution. These domains must be getting smaller in 3 times of their parents. Domain D is covering Yenikapı region in order to obtain more accurate results for tsunami parameters at near shore and inundation zone. The grid model of smallest domain (D) for simulations of tsunami propagation in the European part of İstanbul from Yenikapı to Kumkapı extends from 40.9949°N to 41.0050°N and from 28.9520°E to 29.9794° E.

In the nested simulations, it is important that at least the biggest domain B has to contain the source in the boundary, which is required by the tsunami numerical modeling tool. The tsunami numerical code NAMI DANCE distributes the source into the smaller domains and calculates the tsunami wave parameters.

In high resolution studies, simulations may take very long time depending on the selection of time interval to calculate the results by tsunami numerical model. In order to make the grid size smaller like 1 m, a number of domains have been created and let the numerical model calculate the required tsunami parameters such as inundation, run-up height and the velocity at each point in the grid system. Since the tsunami computational tool NAMI DANCE allows the domains 3 times smaller one

of the other, then at least 5 domains should be created to make the high resolution analysis (90 m > 30m > 10m > 3.3m > 1.1m). This process takes very long computational time like couple of months even with a 64 processor computer. In order to save time it is preferred to run the tsunami numerical model once for the nested domains (B, C, and D) and to obtain water level change at the border of smallest domain (Domain D). Afterwards, a very high resolution (1 m grid size) Domain D is developed using GIS implementation considering buildings, transportation networks and infrastructures. At the final stage, single domain (Domain D with 1 m grid size) simulation using the wave input from the border (computed from nested simulations) is applied.

Table 4: The Coordinates of the nested domains (B, C and D)

The Name of Nested Domain	Grid Size (m)	Coordinates of the Domain
B	90	40.210° – 41.260° N 26.542° – 30.020° E
C	30	40.971° – 41.041° N 28.920° – 29.045° E
D	10	40.9949° – 41.0050° N 28.9520° – 29.9794° E

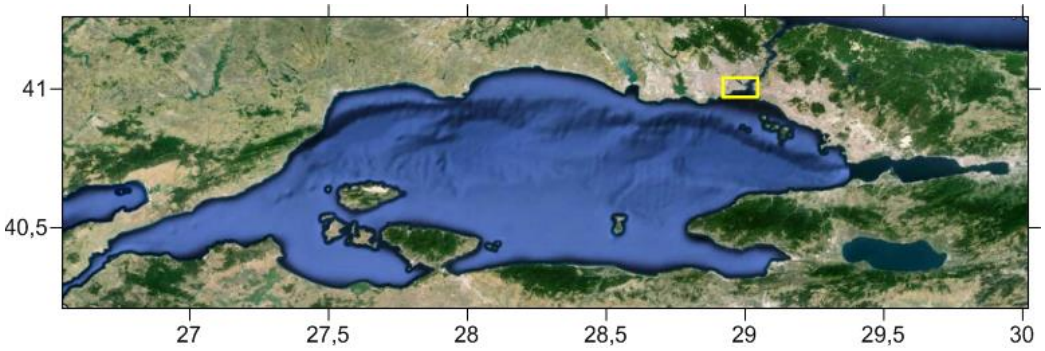

(a)

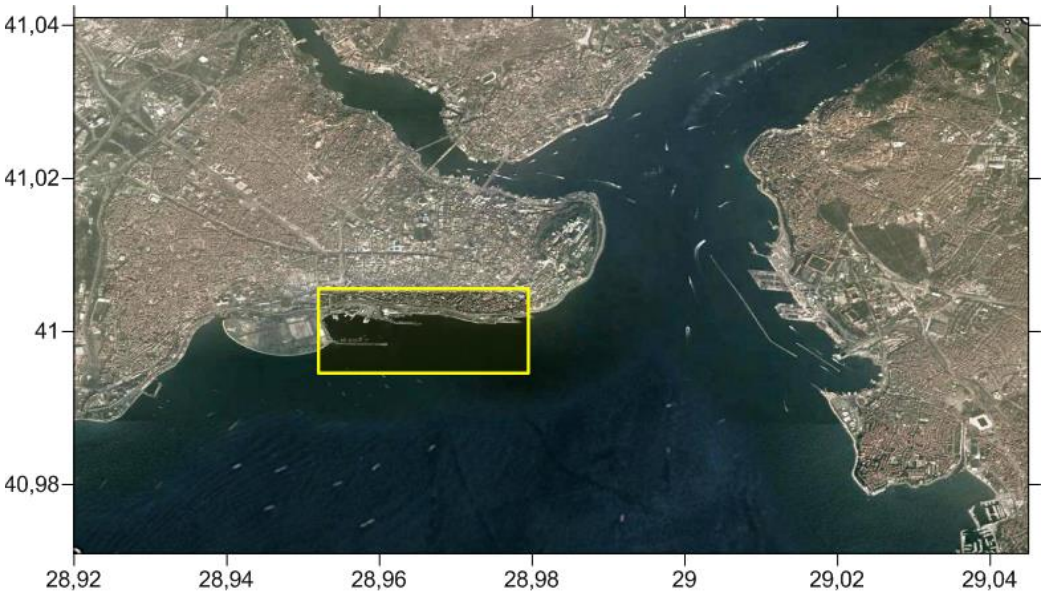

(b)

(c)

Figure 9: The layout of nested domains. (a). The nested domain B, (b). inside C, and (c). inside D.

2.4 Development of High Resolution Topographical and Bathymetric Data with Structures for Fine Grid Simulations at Yenikapı

In order to make higher resolution numerical modeling, necessary implementations for the dataset are performed. The dataset for whole İstanbul region was purchased from İstanbul Metropolitan Municipality (IMM). Two different types of data are used in this thesis. They are: (i) the topographical data in XYZ (longitude, latitude and elevation) format made of 5m spaced points for the whole İstanbul region and (ii) the vector data containing all kinds of building and infrastructural properties. Management of geographical information of dataset and necessary implementations are performed via GIS tools. The data set is analyzed to form a database of bathymetry and topography of the region in coordinates by (i) setting a projection system; (ii) creating digital elevation model (DEM) and adding coordinates, and (iii) doing overlay operations.

There are 3 phases of data processing. The first phase is to develop high resolution bathymetry and topography for tsunami modeling by GIS implementations. In this phase, the coordinates of the shoreline are obtained from Google Earth images and added to the data set. The bathymetric data near the Yenikapı region has also been obtained by digitization of Nautical Charts of Navigation, Oceanography and Hydrography Department from Turkish Navy. The available topographical data obtained from Directorate of Cartography underneath of Department of Housing and Urban Development of İstanbul Metropolitan Municipality (İMM) is converted into a new geodatabase in order to visualize it in GIS tools. ITRF 96-UTM-Zone 35N (Transverse Mercator), is used as the base projection system, Then, a new feature class for rectangular frame is created by using the coordinates of the domain D and with the same projection system. Next, all geographical coordinates and the elevations of the topography data is extracted by the rectangular frame, and converted into WGS-84 datum in order to merge with the vector data governing building and all infrastructures present in Yenikapı.

The second phase is focused on to improve the topographical data by inserting building heights at their locations with a 1 m-spaced grid in order to create

metropolitan topography. To increase the working resolution, available vector data consisting of all buildings and/or structures in the study area are defined as polygons. The corner coordinates and the average heights of each building and/or structures are included in the vector data; however, only corner points are not adequate to interpolate a surface. In order to mitigate interpolation and prevent omission of the small buildings and/or structures, individual polygons are filled up with 1 m regularly-spaced points and hence the number of points in the metropolitan topography are synthetically increased. The average heights of polygons are assigned to all individual points coinciding with respective polygons in given coordinate system and datum (WGS-84), representing buildings and/or structures at the study region. Then, a grid system is created by combining the topographical data and the created point data derived from the available vector data, minimizing interpolation.

The third phase is the vital stage which increases the quality of the input data for accurate tsunami modeling. In this phase, the improved topographical data and the point data produced by the available vector data are overlaid to produce the highest resolution input data for Yenikapı region. Hence, a new digital elevation model (DEM) is generated. Moreover, the new created DEM and the bathymetric data are combined considering the sign (sea +ve, land –ve) for tsunami modeling.

2.5 Nested Domain Simulations

The available bathymetric data obtained from GEBCO (General Bathymetric Chart of the Oceans) of the British Oceanographic Data Centre and the topographic data obtained from ASTER Global DEM with 30 m spatial resolution for Yenikapı region in İstanbul have been analyzed and processed. Then, the bathymetry and topography database are obtained for the input to the tsunami numerical code NAMI DANCE for preliminary nested simulations.

Two preliminary tsunami simulations by inputting PIN and YAN sources are performed. Three nested domains previously selected are given in section 2.3. In

these simulations, tsunami propagation in domains B, C and D are computed simultaneously. The distribution of maximum water elevations in domains B and C at the end of 90 minutes simulation and the tsunami sources PIN and YAN are presented in Figure 10.

It is seen in Figure 10 that there are higher amplitudes near Yenikapı for the YAN source. In fact, the location of YAN source is far from Yenikapı comparing with the location of PIN source. Even if the amplitudes of PIN and YAN sources are similar, the depression plate of YAN source is at north and it causes the leading depression wave propagating towards Yenikapı. According to numerous investigations (Tadepalli and Synolakis, 1996), the leading depression wave causes higher amplification and run-up, comparing to the leading elevation wave of similar amplitude.

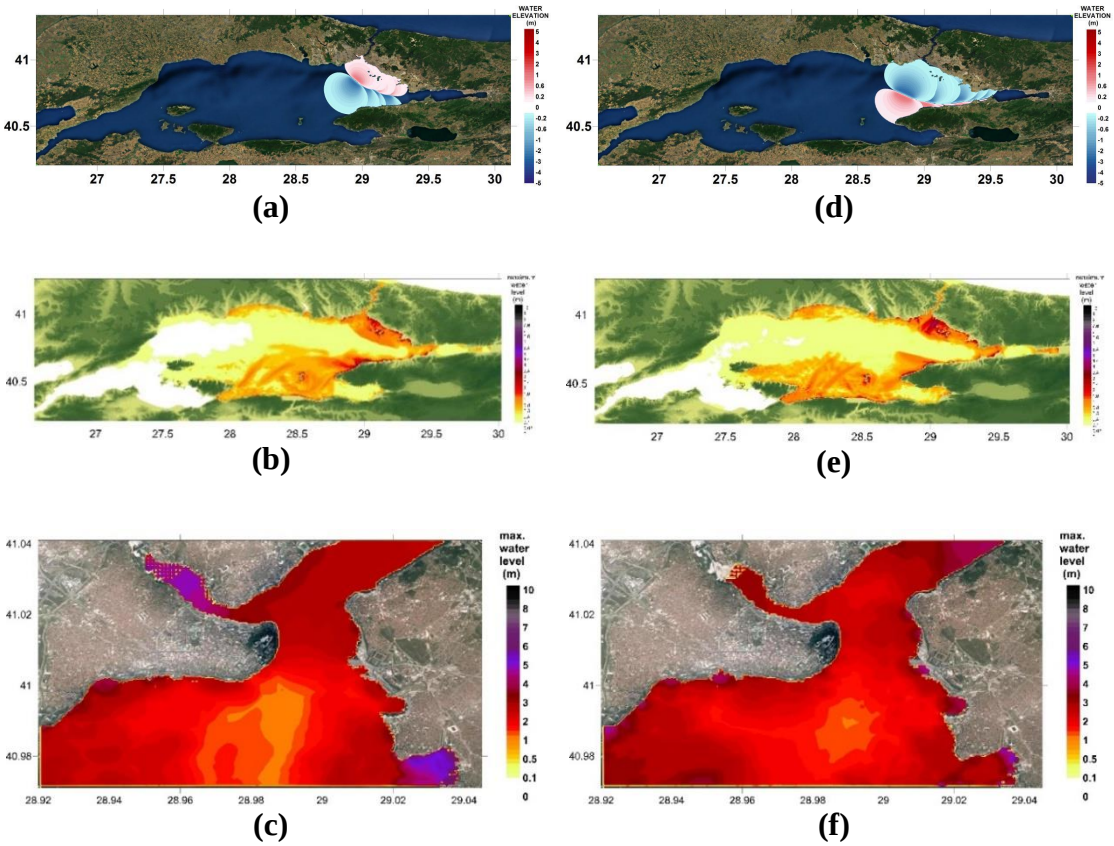

Figure 10: The tsunami source and distribution of maximum water elevations computed at the end of 90 minutes simulations by NAMI DANCE for the tsunami sources PIN (left) and YAN (right). (a-d) The tsunami sources, (b-e) The distribution of maximum water elevations at Domain B, (c-f) The distribution of maximum water elevations at Domain C.

2.6 High Resolution (Grid size, 1m) Single Domain Simulations

The water level change at the southern border of domain D computed from nested simulations for PIN and YAN sources separately are given in Figure 11. The wave at the border of domain D from YAN source (red-line) has leading depression character; however the wave coming from PIN source (blue-line) has leading elevation character. The wave input to domain D (1m grid size) is simulated for 90 minutes duration and all necessary tsunami parameters (mainly maximum water elevations, maximum current speed, maximum flow depth, maximum fluxes) are computed separately for Yenikapı by NAMI DANCE. Among those parameters,

flow depth is one of the major parameter for vulnerability analysis. It is plotted in Figure 12 and Figure 13 as the results of simulations using PIN and YAN tsunami sources.

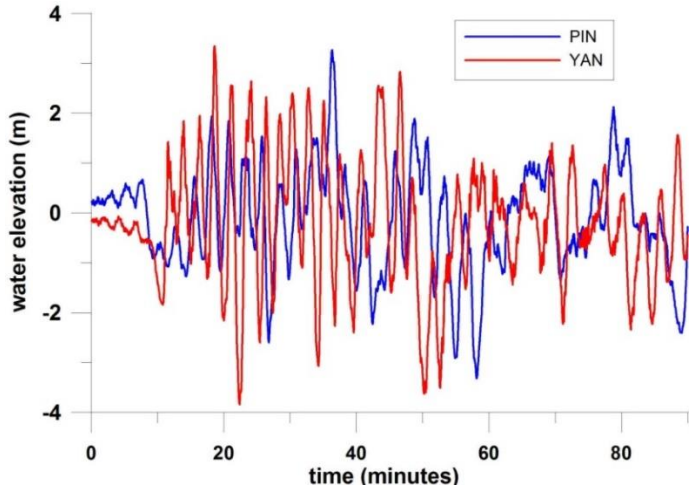

Figure 11: Time histories of water level change at the southern border of domain D computed from nested simulations for PIN and YAN sources

As seen in Figure 12, maximum flow depth exceeds 6 m near the shoreline at east of the Yenikapı Fishery Port; it is represented by purple color according to the simulation of PIN source.

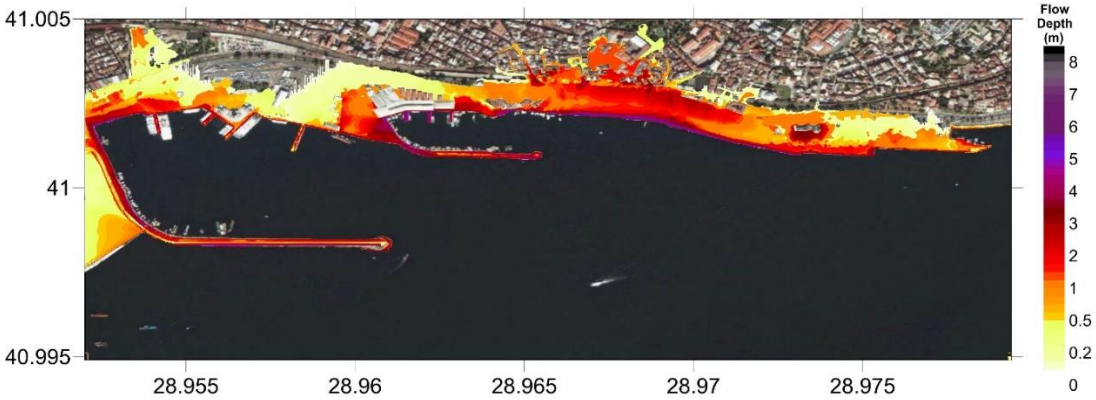

Figure 12: The inundation (flow depth) map of the source PIN

In Figure 13, the distribution of the flow depth computed by the simulation of YAN source is presented. In this simulation, the flow depth exceeds 6 m at not only near

the shore, but also in front of the high historical city wall which prevented water flow and caused accumulation of water volume in front. Hence, higher flow depths are observed in front of the historical wall.

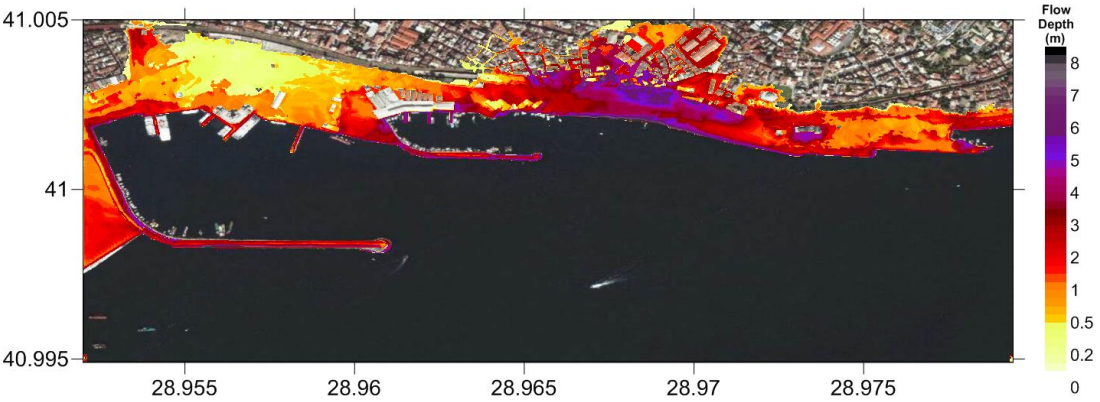

Figure 13: The inundation (flow depth) map of the source YAN

When the results of simulations by PIN and YAN sources are compared, it is observed that tsunami source YAN, causes relatively longer inundation distances and higher flow depths at Yenikapı, than tsunami source PIN. Therefore, the results of the simulation by YAN source (Figure 13) are more critical to use in the tsunami vulnerability analysis. Those results are used in the following chapters.

CHAPTER 3

TSUNAMI HAZARD ASSESSMENT AT YENİKAPI REGION

A recent increased interest in disaster risk is related to a trend in natural hazard sciences where hazard-oriented approaches are shifted to risk assessment. Tsunami risk assessment became more important after 2004 Indian Ocean tsunami. The generic risk approaches have already been applied to the general field of technological risk management (such as in the chemical and nuclear industry) or risk studies related to natural hazards (e.g. floods, earthquakes, tsunamis, storm surges or other extreme events). Tsunami risk assessment is a complex field which requires knowledge from different disciplines (basic, applied and administrative sciences).

The reliability index of 76 events among 134 tsunamis in the Eastern Mediterranean was noticed as “probable” and “definite” in Altınok et al., (2011). It has also been noted that 18 tsunami events are definite among 35 occurrences. Therefore, almost 50 percent of the reported tsunami events are definite.

Tsunami risk assessment for a specific region must focus on vulnerability of not only the structures but also the human evacuation. However, the tsunami assessment from source to the site should also be performed using reliable data and computational tools. In order to develop reliable data of tsunami parameters for vulnerability analysis, the tsunami generation mechanisms, tsunami propagation, coastal amplification and inundation had already studied specifically for Yenikapı region in preceding sections.

3.1 Literature Survey on Geographical Information Systems (GIS) based Multicriteria Decision Analysis (MCDA)

GIS-based MCDA studies are applicable for different studies such as site selection by considering economic, social and environmental and technical relations of the alternatives that are created for decision making analysis. Several different MCDA methods have been used to solve various applications of decision problems. One of the most common methods is AHP (Analytical Hierarchical Process).

Analytical Hierarchical Process (AHP)

AHP is a method developed by Saaty (1980) is a technique to obtain decision alternatives with a mathematical structure. The main aim is to obtain weights through pairwise comparisons of attributes and in addition to find rank values through pairwise comparisons of alternatives for each attribute (Marshall and Oliver, 1995). The method is based on three principles: decomposition, comparative judgment and synthesis of priorities. In the AHP, the first step is that a complex decision problem is decomposed into simpler decision problems to form a decision hierarchy (Erkut and Moran, 1991).

AHP procedure is implemented by 3 major steps:

1. *Development of the AHP Hierarchy:* In hierarchy, the top level is the ultimate goal of the decision. The hierarchy decreases from the general to more specific. Each level must be linked to the next higher level. The hierarchical structure is composed of four levels: goal, objectives, attributes and alternatives. The alternatives are determined and produced in GIS database. Each layer includes the attribute values which are assigned to the alternatives (e.g. cell or polygons). When the decomposition principle is completed, cardinal rankings for objectives and alternatives are required. This process is performed by the using pairwise comparison because of reducing the complexity of decision making.

2. *Comparing the Decision Elements on a Pairwise Base:* Pairwise comparisons are implemented in 3 steps:
    i. Development of a comparison matrix at each level of the hierarchy,
    ii. Computation of the weights for each element,
    iii. Estimation of the consistency ratio.

The weights are computed by using eigenvector, which is strongly recommended. To determine the priorities derived from a positive reciprocal pairwise comparison judgment matrix, the principle eigenvector is necessary (Saaty, 2003).

Construction an Overall Priority Rating: The final step is to determine the relative weights of the levels obtained in the second step to produce composite weights. This is done by means of a sequence of multiplications of the matrices of relative weights at each level of the hierarchy. The overall score R_i of the i_{th} alternative is the total sum of its ratings at each of the levels and is thus computed in the following way:

$$R_i = \sum_k w_k \, r_{ik} \tag{3.1}$$

where w_k is the vector of priorities associated with the k_{th} element of the criterion hierarchical structure, $\Sigma \, w_k = 1$; and r_{ik} is the vector of priorities derived from comparing alternatives on each criterion (Equation 3.1). The most preferred alternative is selected by identifying the maximum value of R_i (i= 1, 2, ..., m).

The consistency ratio (CR) measures the admissible level of consistency in the pairwise comparison. If CR is less than 0.10, the ratio indicates that consistency is reasonable. However, if CR is equal and more than 0.10, the ratio indicates the inconsistent judgment (Malczewski, 1999).

Tammi and Kalliola (2004) were performed two case studies in two different European seas, one is focusing on artificial reef in the Mediterranean Sea and the other is translocation of aquaculture in Baltic Sea. This study is conducted using GIS-based MCDA to be able to create structure and to make assessment for solving marine planning decision problems. Analytical decision frame works have been

produced by considering their regional characteristics and the problems sourced by nature separately. The available data were spatially determined and enhanced using GIS software. In Aegean Sea case, modeling, interpolation and resampling methods are used to convert into a data which has 25m resolution. The spatial parameter layers were prepared and weight values have assigned to each parameter as a procedure of AHP, using a popular decision support system. For normalization of the weighted values, the Eucledean distance was used. In order to prevent uncertainty in the decision making analysis, seconder weights depending on the variance of ideal values were integrated into the distance metric. The weighted values have been normalized and the final output has been obtained as a continuous raster surface by joint use of GIS and MCDA. In the Archipelago Sea case, the maps produced previously have been masked to exclude non-required areas. Maximum aquaculture production capacity has been computed. Five potential production consolidated sites have been ranked, applying discrete MCDA method for determining ordinal rankings on a scale 1 to 5. Production of comparison layers were produced using GIS. At the end, a suitable ordinal ranking score has been obtained for each site. Researchers were applied spatial MCDA methods by considering marine spatial planning and they discussed the results.

One of GIS-based MCDAs was carried out by Şener et al., (2006) for selection of appropriate landfill site. Authors discovered that there are many important factors like regulations, environmental, socio-cultural, engineering and economic factors which must be considered when evaluating potential landfill sites for disposal of solid wastes. For this study, authors have determined the possible sites in the region of south western Ankara by integration of MCDA and GIS applications. 16 layers (topography, roads, geology etc.) which may affect the site selection have been prepared as inputs and decision making model (simple additive weighting (SAW) and analytic hierarchy process (AHP) to analyze the dataset were performed in GIS environment. For SAW method, weight and rank values in the range of 0-5 were assigned to layers and classes of each layer, and for AHP, the values change in the range of 0-50. Depending on weight and rank values, the site selection maps were generated. Authors noticed that the results of both MCDA models have been

compared depending on a comparison matrix and although the results were found compatible, AHP gave more consistent results than SAW.

The purpose of the work by Kolat et al., (2006) was to generate geotechnical microzonation model by integration of GIS tools and MCDA for obtaining the results. The aim of the development of microzonation model is to present an effective solution to find out new residential areas. Authors stated that after the selection of the city center of Eskişehir as study area, 6 main layers like liquefaction potential, flood susceptibility, slope etc. have been prepared from the three various data sets containing topographical base maps, lithological maps and geotechnical boreholes. The rank and weight values have been allotted to the layers and classes respectively, by the application of two different decision models (AHP and SAW). Additionally, authors obtained geotechnical microzonation maps from the decision models by considering hierarchical structures to indicate the possible areas on created maps. The comparison of the two decision models, authors recommended the AHP model because of its higher consistency.

Another study has been performed by Kolat et al., (2012), where they have developed geotechnical microzonation model for Yenişehir (Bursa, Turkey) by using GIS-based MCDA. It has been stated that the area is at a seismically active region. The purpose of the study helped further improvement on the geotechnical microzonation model by considering the appropriateness of the residential zone. Authors collected the previous studies performed for Yenişehir in order to use them in these seismic risk evaluations. Then, they generated the similar model previously developed for Eskişehir region. Differently from the previous study, Analytical Hierarchical Process (AHP) method has been selected as the decision model to assign weight values to the determined layers. These layers were liquefaction, soil amplification and distance to stream maps.

Rikalovic et al., (2014), carried out another site selection study by using GIS-based MCDA. It is aimed to find out the most suitable industrial site. Geographical data takes a role in decision making process. Authors stated that as GIS tools uses the real-world coordinates to provide a better way of viewing and exploring the data, it

has been preferred for this spatial analysis. Besides, GISs are the systems which worked jointly with the other systems and methods like decision making systems to increase the accuracy and the quality of the analysis. Authors developed a model and followed its steps respectively to receive efficient and accurate result as follows: defining the problem, focusing on analyzing of the alternatives, determination of the factors and constrains, standardization of the factors/criterion scores (after creation of rating scale), assignment of decision variable, generating alternatives by GIS approach, assignment of weight and rank values to the layers and classes, aggregation of the criteria, validation of the results sensitivity and recommendation for decision making. Their model allowed them appropriate site selection for industrial areas. .

Niaraki and Malczewski, (2014), have conducted another study that focused on the effect of the complex decision task on the data acquisition strategies in a GIS-based MCDA. They used Multi-Criteria Spatial Decision Support System (MC-SDSS) for online parking site selection to test complexity, choosing a district in Tehran city, Iran.

Malinowska and Dziarek, (2014), were conducted a study for cave-in occurrence using AHP and GIS. In this study, the risk of existence of discontinuous deformation on the surface is estimated. Qualitative and quantitative factors causing discontinuous deformation have been determined to estimate potential sinkhole zones. The results are validated and verified. The locations which have actual and high-risk potential deformation were compared. The results related with the evaluation of sinkhole hazards have been presented.

A MCDA-GIS based model was developed by Modica et al., (2014), for the site suitability evaluation of traditional grape varieties. Montonico region located at south of Calabria in Italy has been selected as a case study. Criteria, which are responsible from the physical land suitability, have been determined. Structuring and modeling have been performed using GIS-based MCDA procedure. The results obtained by the model were validated and verified by comparing the real geographical conditions. The results and the real conditions are found compatible to each other.

3.2 Vulnerability Assessment at Yenikapı Region

In the previous chapters, the database is processed and numerical model, NAMI DANCE is applied to compute the tsunami parameters. Among those parameters, flow depth at inundation zone is selected to implement tsunami magnitude for vulnerability analysis. This chapter covers details of vulnerability analysis by implementing by implementing MCDA to GIS for Yenikapı.

3.3 The Available Datasets used for computing Locational Vulnerability and Evacuation Resilience at Yenikapı Region

There are 2 available datasets used in the determination of tsunami vulnerability assessment at Yenikapı. The first one is the vector dataset of the entire İstanbul region (Figure 14). It is prepared by İstanbul Metropolitan Municipality (IMM) and dated back to 2006. The raw dataset is composed of hundreds of points (e.g. utility poll, single graves, billboards, etc.), polylines (e.g. retaining walls, walking-tracks, scarps, etc.) and polygons (e.g. decorative pools, greenhouses, penthouses etc.) representing all available metropolitan structures and infrastructure (Figure 14 and Figure 15). The available vector data is cropped into study region and necessary modifications are performed to select and use the most appropriate vector element attributes. The second available dataset is DEM with 5m resolution, created from aerial photogrammetric techniques based on 2006 data and obtained from İstanbul Metropolitan Municipality (IMM).

Figure 14: The Yenikapı view of the vector data obtained from IMM.

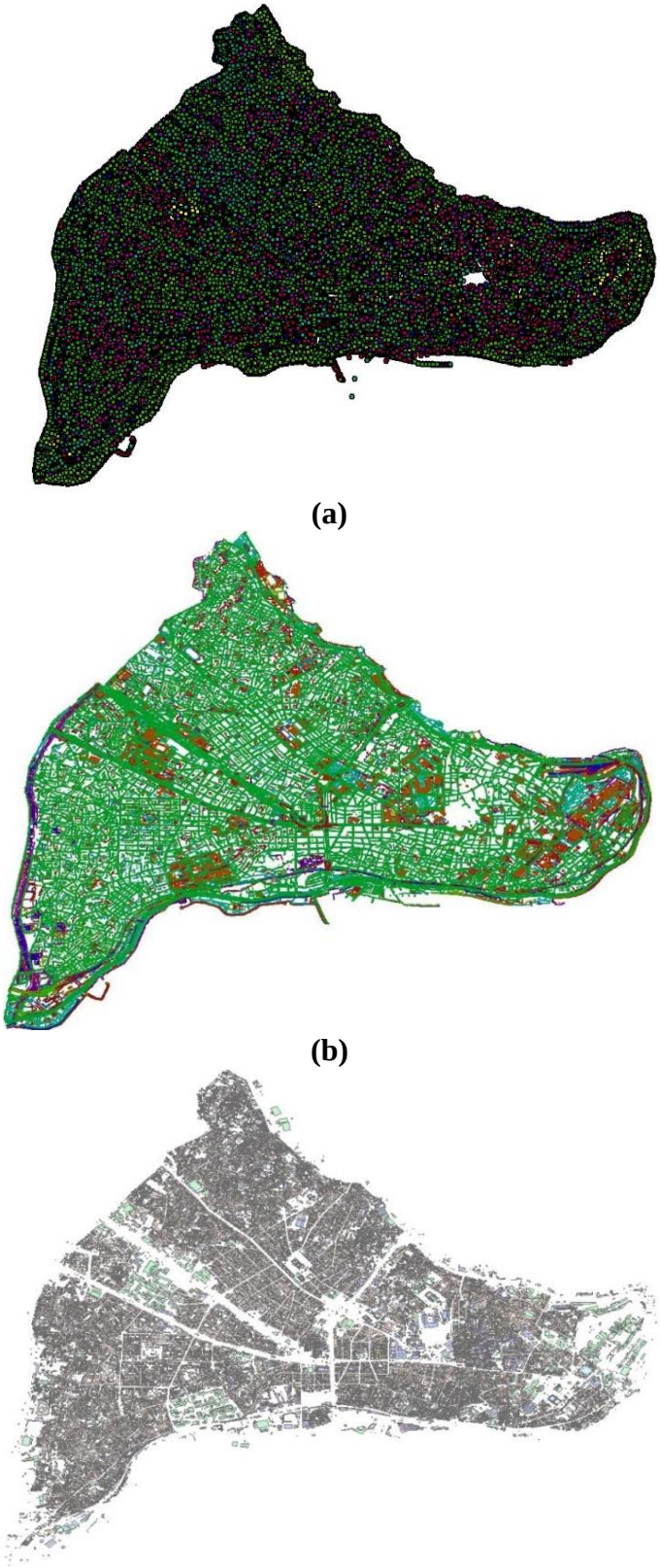

(a)

(b)

(c)

Figure 15: The raw vector data composed of points (a), polylines (b) and polygons (c) obtained from İstanbul Metropolitan Municipality (IMM).

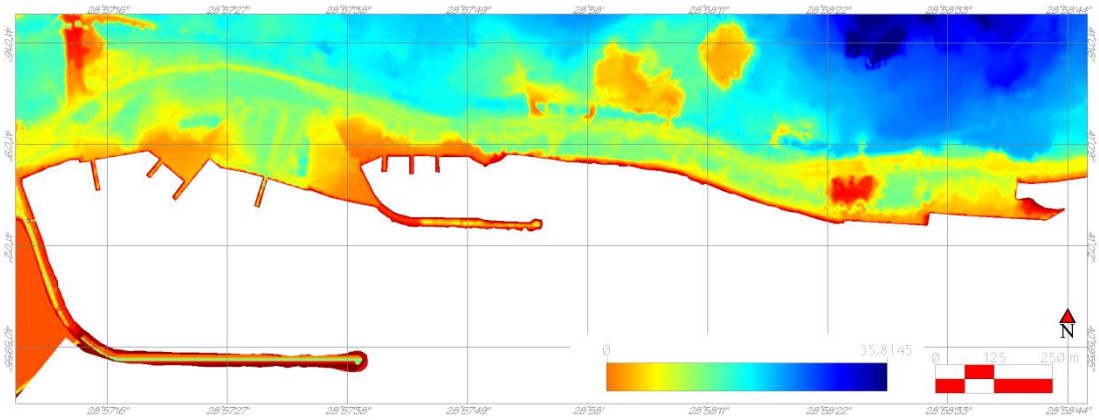

Figure 16: Digital elevation model (DEM) of Yenikapı with 5 m resolution

Regarding context of two available sources, it is decided to produce 8 parameters as vulnerability and resilience related layers for MCDA. While the IMM vector data allows creating 6 layers, 2 more layers are created from DEM. Vector data yields in distance from shoreline, geology, metropolitan use, distance to building, distance to road network and distance within flat areas. Whereas DEM serves as source for topographic slope and vertical elevation from mean sea level.

In this study, these layers are particularly categorized into 2 different categories. They are (i) the spatial distribution of vulnerability due to distance to shoreline, geology, elevation and metropolitan use of the location, and (ii) the spatial distribution of resilience based on ease of evacuation due to distance to building, slope, distance to road network and distance to flat area.

The hierarchical structure used in preparation of the vulnerability map is given in Figure 17. It is used to allot the weight and rank values to the layers and classes of each thematic map in the AHP method.

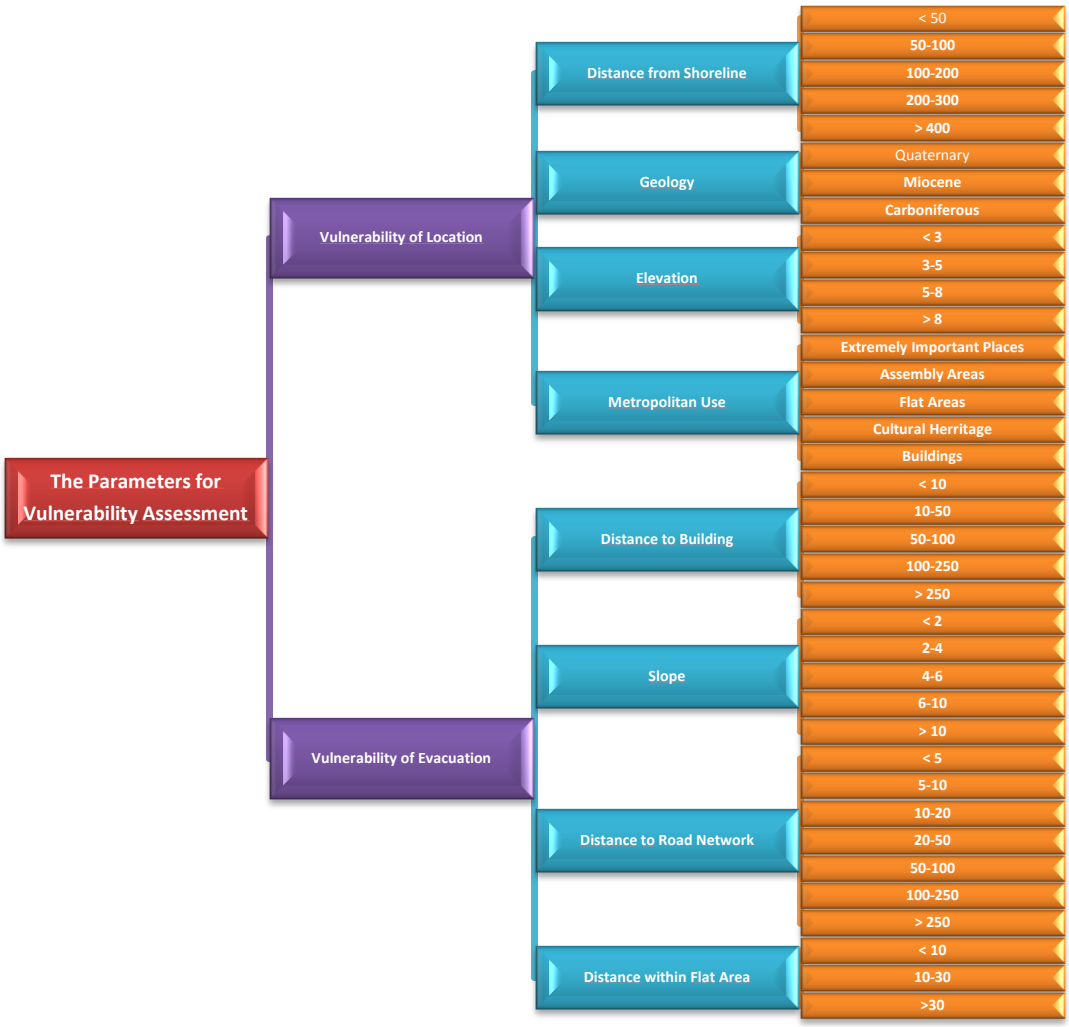

Figure 17: The hierarchical structure used in the preparation of the vulnerability maps.

3.4 Assumptions of for the Locational Vulnerability and Evacuation Resilience Assessments

A number of assumptions are made throughout the MCDA implementations, which are listed below:

- The earthquake is assumed as a precursor of tsunami which may warn people to consider arrival of a tsunami soon (enough time to move to safer locations).
- The buildings are considered rigid and undamaged by the effect of Tsunami.

- It is assumed that the vertical evacuation is possible in every building and the number of the floors are higher than 1 except prefabricated buildings.
- Day and night populations are assumed as constant.
- It is supposed that tsunami waves arrive at the same time at all locations of Yenikapı shoreline in study area (about 2 km portion of Yenikapı shoreline).
- The duration of inundation is governed by period of tsunami wave. According to the results of simulations using critical scenario in deterministic approach, the period of tsunami waves is estimated approximately 10-15 minutes. In the vulnerability analysis, the duration of the tsunami inundation is sufficiently long.

3.5 Vulnerability Analysis at Location

3.5.1 AHP Analysis for Vulnerability and Production of Vulnerability Maps

The tsunami vulnerability at any location in Yenikapı is determined by comparing the topographical and metropolitan parameters. These parameters are determined as metropolitan use, geology, elevation and distance from shoreline.

In this section, input datasets are manipulated and appropriate parameter layers are produced to construct the MCDA framework for calculation of the vulnerability score at location in Yenikapı.

In contrast to the presence of very detailed spatial data; some part of the data are old and hence updated manually from Google Earth images, available reports and field studies. The outlines of the prefabricated buildings behind İDO-İstanbul Sea-bus Terminal (the glass-wall building), the entrance of the tube-tunnel railway and the wedding-ceremony hall are updated manually to the metropolitan use vector data. Since the huge 715,000 m^2 meeting area located at the western side of the study area was not constructed in 2006, it is not covered by the available vector dataset. Thus,

the shoreline and the meeting area are updated digitizing, regarding the current Google Earth imagery.

The input data and their relevant parameter maps/layers are as follows:

3.5.1.1 Metropolitan Use Layer

The entire attributes of metropolitan use vector data are analyzed and grouped into meaningful units by gathering similar type polygons. Hereby 23 descriptive units which represent buildings and/or structures are produced from hundreds of data. An attribute table is created for the vector data grouping the metropolitan use against tsunami vulnerability (Table 15).

Table 5: Attribute table of descriptive units of the metropolitan vector data.

No	Structure and/or Building Type	Groups by considering possible tsunami vulnerability
1	Prefabricated buildings	Extremely Important Places
2	Gas stations	Extremely Important Places
3	Electricity transformers	Extremely Important Places
4	Pedestrian underpasses	Extremely Important Places
5	The glass-wall building (İDO-İstanbul Sea-bus Terminal)	Extremely Important Places
6	The entrance of the Eurasia (Avrasya) Undersea Highway Tunnel	Extremely Important Places
7	Ruins	Extremely Important Places
8	Religious facilities	Assembly Areas
9	Sports facilities	Assembly Areas
10	Schools	Assembly Areas
11	Suburban railways	Flat Areas
12	Asphalt roads	Flat Areas
13	Parking places	Flat Areas
14	Others (including green fields and medians)	Flat Areas
15	Stationary city walls	Cultural Heritage
16	Demolished city walls	Cultural Heritage
17	Historical places	Cultural Heritage
18	Factories	Buildings
19	Small-scaled production center	Buildings
20	Under construction buildings	Buildings
21	Residential places	Buildings
22	Wedding ceremony halls	Buildings
23	Commercial buildings	Buildings

All kind of buildings and structures located at the study area are classified into 5 main groups. These are extremely important places (e.g. prefabricated building, gas station, electricity transformers, pedestrian underpasses, İDO- İstanbul Sea-bus Terminal (the glass-wall building), the entrance of the Eurasia (Avrasya) Undersea Highway Tunnel, ruins etc.), assembly areas (e.g. religious facility, sports facility, school, wedding-ceremony hall etc.), flat areas (e.g. asphalt road, suburban railway, parking places, others (including green fields and medians) etc.), cultural heritage (e.g. stationary city wall, demolished city wall, historical places/buildings etc.) and buildings (e.g. factory, small-scaled production center, building under-construction, residential places/private homes, wedding ceremony hall, commercial building etc.). Type or usage of each building is also considered separately while categorizing built environments because of their relation with vulnerability. In the ranking process, the higher population of the possible locations such as assembly areas is also taken into account for estimation of the vulnerability score of the selected area.

According to the observations from the site visit, there are very few wooden buildings located nearby suburban railway (Figure 18) and 5 prefabricated buildings whose location is behind of the glass-wall building which is the only one building covered by glass (Figure 19 and Figure 20). This is why; it is not feasible to classify the buildings by their construction materials or to their resistivity to waves like in the study of Dominey-Howes and Papathoma (2007). Moreover, age, design and the interior conditions of the buildings are not considered because of the lack of data.

The map of metropolitan use is presented in Figure 21, where red, blue, green, purple, yellow colors represent extremely important places, assembly areas, cultural heritage, flat areas and buildings. The critical areas are prefabricated buildings, gas stations, electricity transformers, pedestrian underpasses, glass-wall building and the entrance of the Eurasia Undersea Highway Tunnel, and ruins.

(a)

(b)

Figure 18: Examples of few wooden buildings located at Yenikapı region.

Figure 19: A view of the prefabricated buildings at Yenikapı.

Figure 20: A view from back side of İDO-İstanbul Sea-bus Terminal (the glass-wall building).

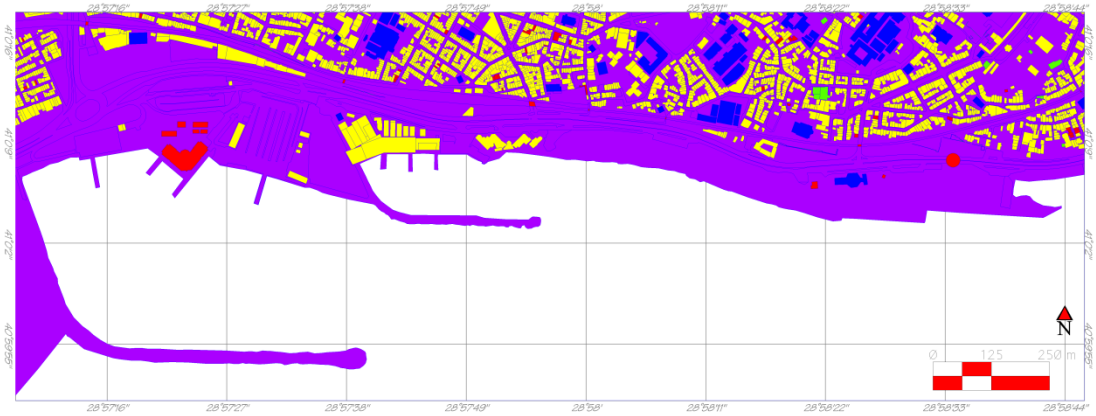

Figure 21: The parameter map of the metropolitan use layer. Extremely important places: red, Assembly areas: blue, Cultural heritage: green, Flat areas: purple, Buildings: yellow

3.5.1.2 Geology Layer

Tsunamis are generated by mostly earthquakes at inter-plate subduction areas. The resistivity of the land is related with the geology. Once the stabilities of geological units are altered by lateral or vertical forces, unwanted slope instabilities, ground deformations, liquefactions etc. might occur. These weakened geological materials can easily be dragged into the sea while creating extra debris, increasing the damage.

IMM has conducted a project, to produce microzonation maps of İstanbul. Among these maps, geological, hydrogeological, structural geology, ground shaking, liquefaction hazard, flooding and inundation, average shear wave velocity, fundamental period, resonant frequency, site amplification and land suitability maps at different scales changing between 1/1000 and 1/5000 which are related to several soil risks. The representative maps are presented online with scales 1/40000 or greater (Figure 22). They are available in IMM website and used in this study by georeferencing the map in the appropriate coordinate system. Then, the geology map is created by retracing and rasterizing the map in GIS environment.

The legend guides to classify the geological units regarding their contents and ages. There are 2 dominant formations, namely Carboniferous Trakya and Miocene Çukurçeşme formations at around Yenikapı. Additionally, around Yenikapı port, in addition to valley alluviums, a part of the sea has been filled up with anthropogenic Quaternary alluvial sediments.

In this study, the geology layer is created by grouping the formations according to their behavior during earthquakes. Their geotechnical behaviors during an earthquake have been elaborately studied in various IMM studies. By considering the closer view of the exact area seen in Figure 23, all natural or anthropogenic unconsolidated deposits are considered as Quaternary alluvium. The others defined in the geology layer are Miocene Güngören Formation and Carboniferous Trakya Formation called as Miocene and Carboniferous respectively to generate the classes mentioned in following sections of the study (Figure 24).

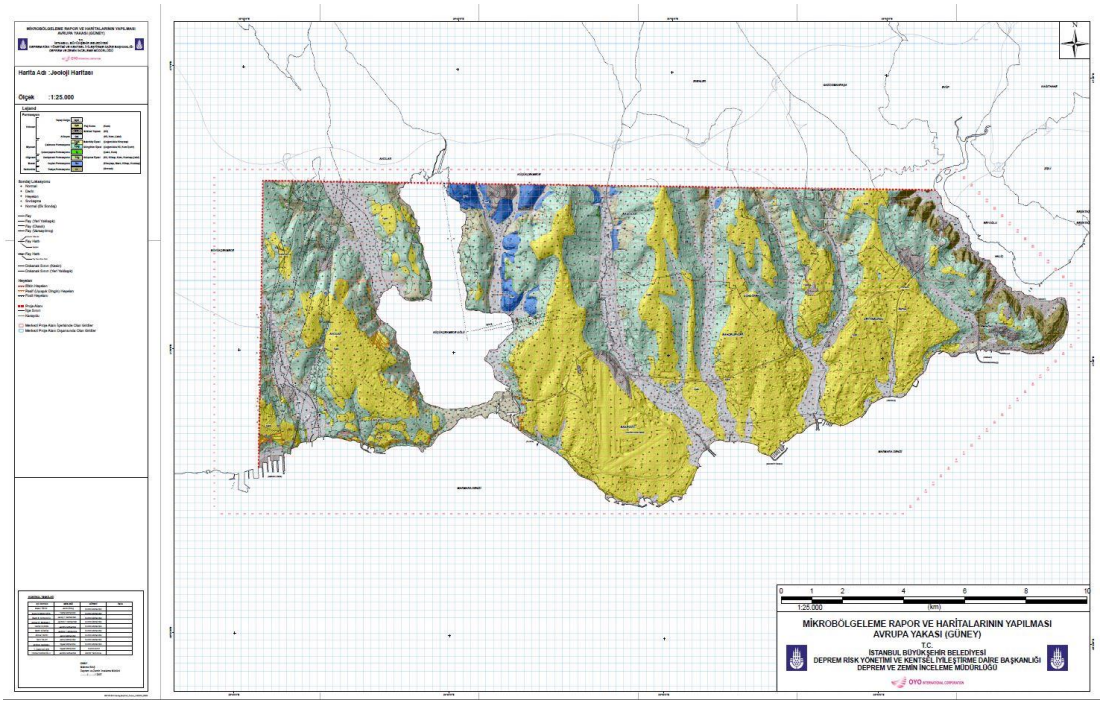

Figure 22: The representative map of geology at 1/40000 scale (İstanbul Metropolitan Municipality, 2015)

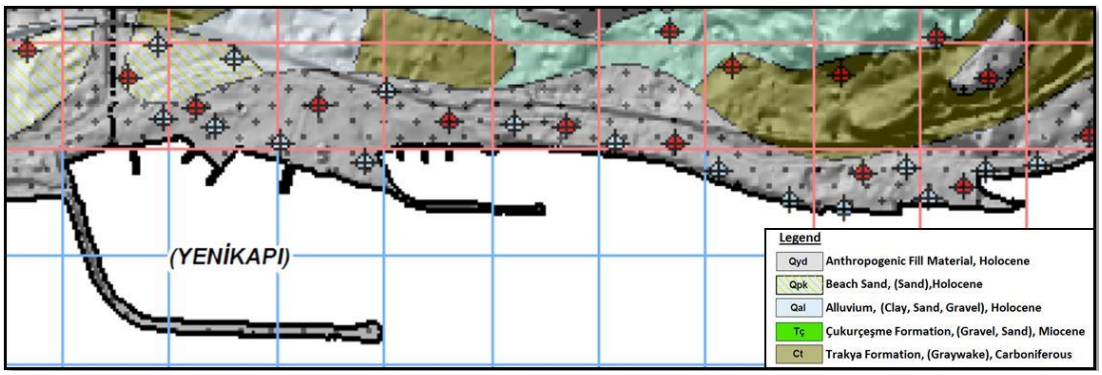

Figure 23: The geology map of the exact study area in a closer view (extracted from İstanbul Metropolitan Municipality, 2015)

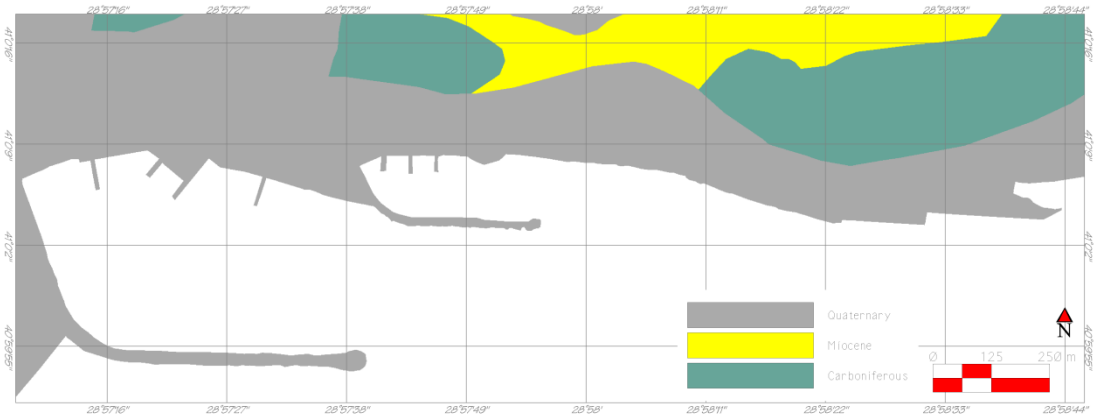

Figure 24: The parameter map of the geology layer.

Additionally, the largest port of the Byzantium period, Theodosius, is placed at Yenikapı. It is established at the mouth of the Bayrampaşa Stream. This stream comprises of the combination of the small stream and floodwaters at the high elevated area except the ancient city walls. It starts from the Sulukule Gate, flows through the city walls and flows into the Sea of Marmara from Yenikapı. The length of the main valley generated by the stream is 3.5 km. This old valley is changed and drained entirely due to immigrations by unplanned urbanization in 1960s (upper left corner of the study area). According to the ancient reports, because of the transgression of the sea about 5000 years ago, the port of Theodosius port was submerged. However, depending on the current archeological excavations, it was used as a port after A.D. 300-400. The port was completely filled up in A.D. 1200, with the increase of Bayrampaşa Stream debris and sea deposits, and the anthropogenic wastes coming from the north settlements because of the increase of the settlements (Erel et al., 2009).

3.5.1.3 Elevation (DEM) Layer

When tsunami comes to a shore, standing at the higher ground will keep the coastal buildings, structures and infrastructures at safe, comparing with the low settled built environments. This is why, it is important to know how the elevation of the coastal area changes from sea level. The land elevation layer is one of the significant parameters to determine the vulnerability of the buildings and the other structures.

The terrain elevation dataset produced by aerial photogrammetric techniques in 2006. The resolution of the data set is in 5 m pixel size. The pixel size is reduced into 1 m by resampling the DEM. It is also enhanced to produce a descriptive layer for tsunami vulnerability assessment. The resolution of the dataset is in 5 m pixel size. The pixel size is artificially increased into 1m by resampling the DEM, in order to make it coherent with the building (metropolitan) topography that had been used in calculation of numerical tsunami models.

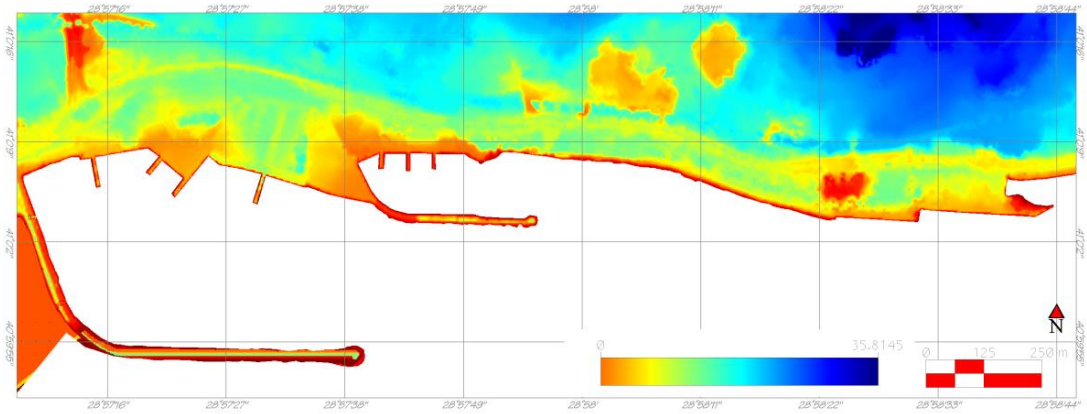

Figure 25: The parameter map of the elevation (DEM) layer

3.5.1.4 Distance from Shoreline Layer

In case of any tsunami threat, it would be good to be away from shoreline. The structures nearby shoreline will be in danger. Independent of the resistivity of the buildings and/or structures depending on the material type, the closeness to the shore will affect vulnerability negatively. Hence, the distance from shoreline is taken as a

parameter to determine the vulnerability.

This layer is generated from the vector form of the shoreline frame (Figure 26) of the study area. The distance from shoreline for each point inside of the boundary is calculated with the conversion of the vector data into raster data by using GIS analytical functions (Figure 27). In this rasterization process to generate the new layer, 1m as raster size and 32 bit floating as raster type are selected for the output.

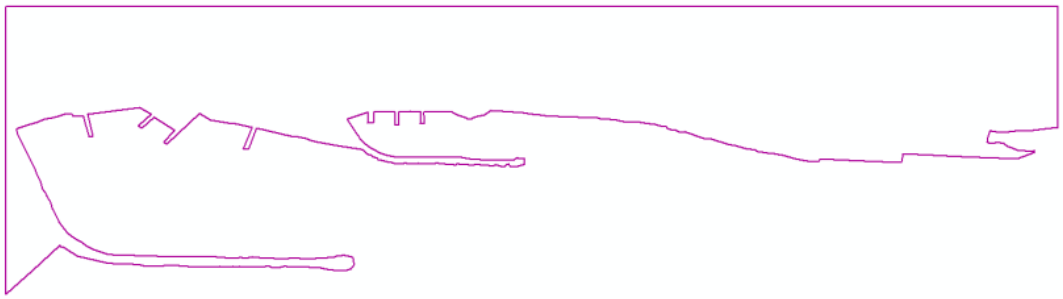

Figure 26: The shoreline frame.

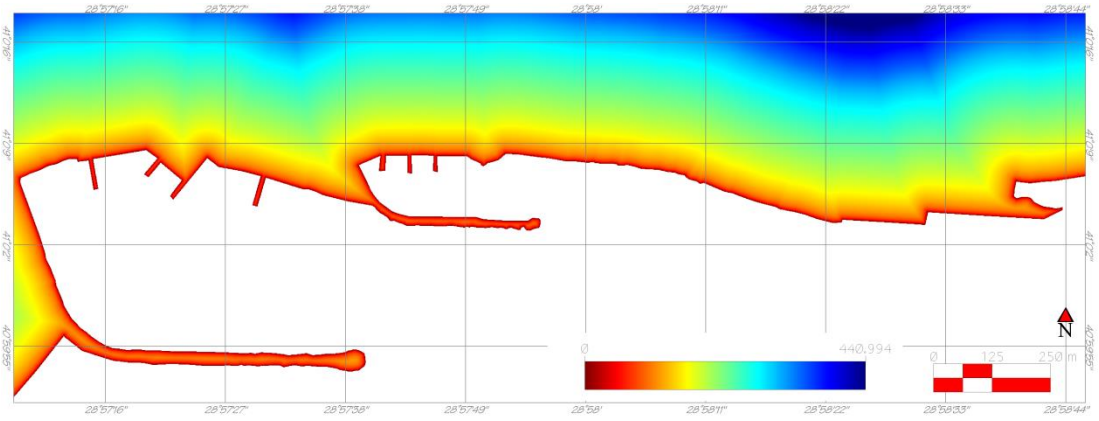

Figure 27: The parameter map of the distance from shoreline layer.

3.5.2 Creating AHP Framework and Final Map Production for Locational Vulnerability Score

The parameter maps generated in the previous section (3.5.1.) will be used in the MCDA process to calculate the locational vulnerability. AHP provides to compare decision making alternatives in mathematical structure. The relative vulnerabilities of 4 layers are identified comparatively by engineering judgments, regarding the intensities of the weight values on Saaty's rating scale (Table 6). While assigning weight values to each layer pairwise comparisons are performed (Table 7). The rank values within each layer are given by experts regarding their appropriate tsunami vulnerability conditions.

Table 6: Saaty's Rating Scale (Saaty, 1990).

Weight/Rank	Intensities
1	Equal
3	Moderately dominant
5	Strongly dominant
7	Very strongly dominant
9	Extremely dominant
2, 4, 6, 8	Intermediate values
Reciprocals	For inverse judgments

Table 7: The pairwise comparison matrix for calculation of locational vulnerability.

Feature	Metropolitan Use	Geology	Elevation	Distance from Shoreline
Metropolitan Use	**1**	1/4	1	1/4
Geology	4	**1**	2	1/2
Elevation	1	1/2	**1**	1/4
Distance from Shoreline	4	2	4	**1**

The logical explanation of the comparison matrix table while using the assigning values is follows:

• The metropolitan use layer has equal importance with the elevation layer. However, the geology and distance from shoreline layers are moderately-strong dominant prevalence against the metropolitan use.

• The geology layer has moderate-strong and equal-moderate prevalence against the metropolitan use and elevation layers, respectively. However, the distance from shoreline layer has equal-moderately dominant prevalence against the geology layer.

• The elevation layer has equal importance with the metropolitan use layer. Additionally, the geology layer and the distance from shoreline layer has equal-moderately and moderately-strong prevalence against the elevation layer.

• The distance from shoreline layer has moderate-strong, equal-moderate and moderate-strong prevalence against metropolitan use, geology and elevation layers, respectively.

The weight values are computed and the consistency ratio is estimated by AHP software (Table 8). Since the consistency ratio is less than 0.10 with the value of 0.0255, the AHP framework is found to be valid and consistent.

HP allows evaluating weight values (Janssen, 1992; Kolat, 2004). Comparison matrices of the each class are prepared and the results are calculated by GIS tools, creating scripts. The alternatives and their rank values are presented in Table 9 to Table 12 and their final maps are also given in Figure 28 to Figure 31.

Table 8: The computed weight values of the locational vulnerability.

Relative Weights	**By weight order**
Distance from Shoreline	0.4833
Geology	0.2917
Elevation	0.1208
Metropolitan Use	0.1042
Consistency Ratio	0.0255 **(Acceptable!)**

Table 9: Classes of the distance from shoreline layer.

Distance from Shoreline	Vulnerability class	Ranking	Ranking (standardized)
w: 0.4833	< 50	1	0.1
	50 - 100	2	0.2
	100 - 200	3	0.3
	200 - 300	6	0.6
	300 - 400	9	0.9
	>= 400	10	1

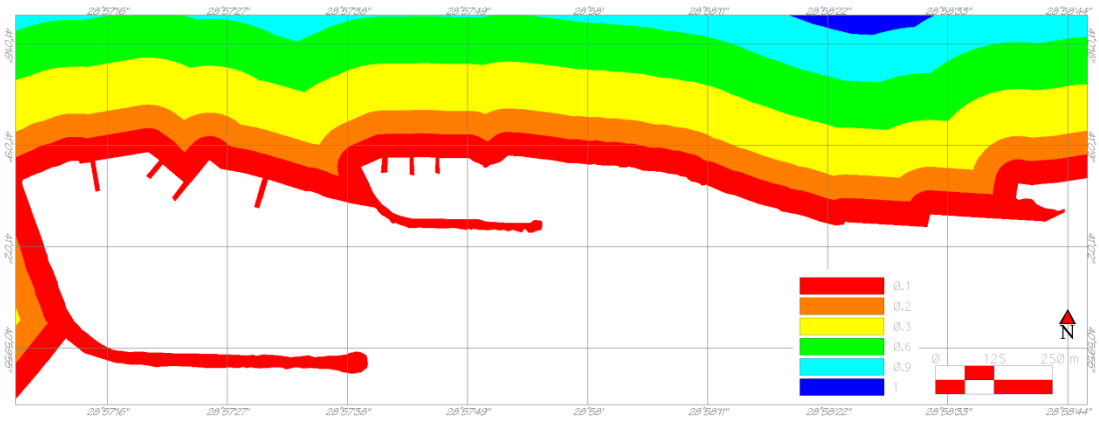

Figure 28: Ranked map of distance from shoreline layer

Table 10: Classes of the geology layer.

Geology	Vulnerability classes	Ranking	Ranking (standardized)
w: 0.2917	Carboniferous	10	1
	Miocene	3	0.3
	Quaternary	1	0.1

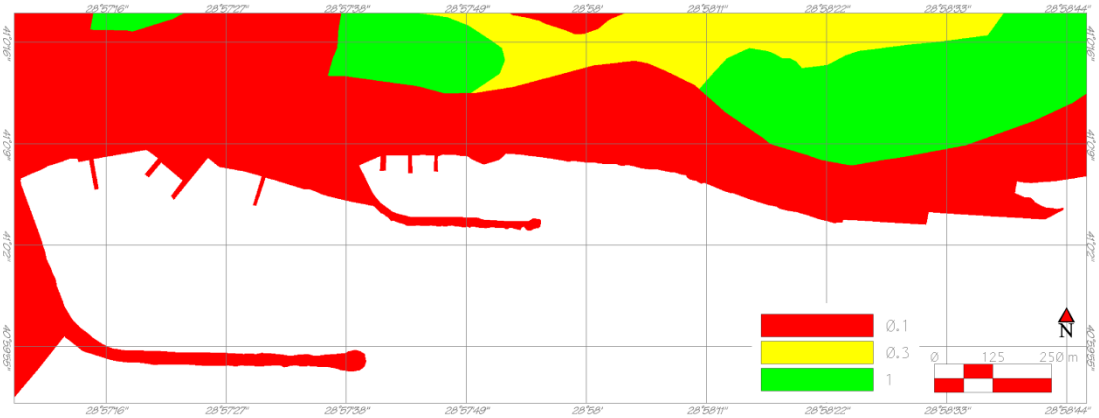

Figure 29: Ranked map of geology layer.

Table 11: Classes of the elevation (DEM) layer.

Elevation	Vulnerability classes	Ranking	Ranking (standardized)
w: 0.1208	< 3	1	0.1
	3 - 5	5	0.5
	5 - 8	8	0.8
	>= 8	10	1

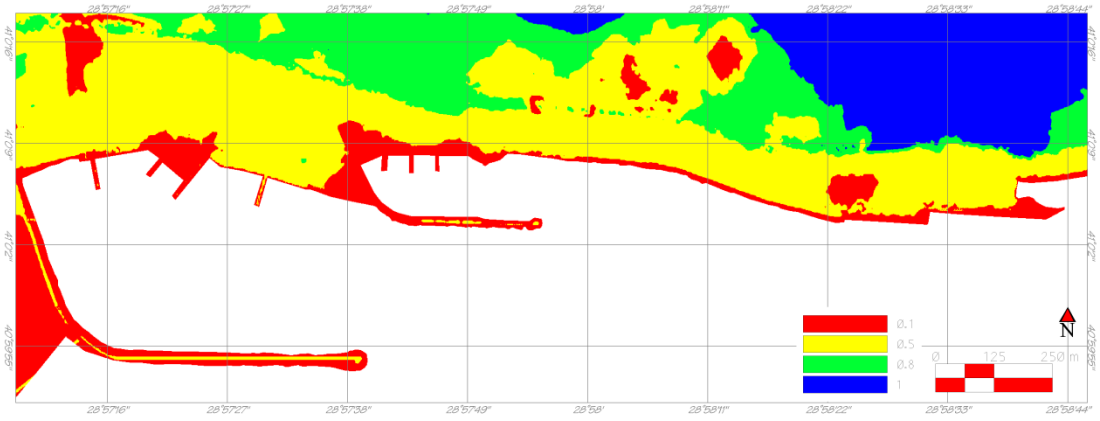

Figure 30: Ranked map of the elevation layer.

Table 12: Classes of the metropolitan use layer.

Metropolitan Use	Vulnerability class	Ranking	Ranking (standardized)
w: 0.1042	Extremely Important Places	1	0.1
	Assembly Areas	2	0.2
	Cultural Heritage	3	0.3
	Flat Areas	4	0.4
	Buildings	10	1

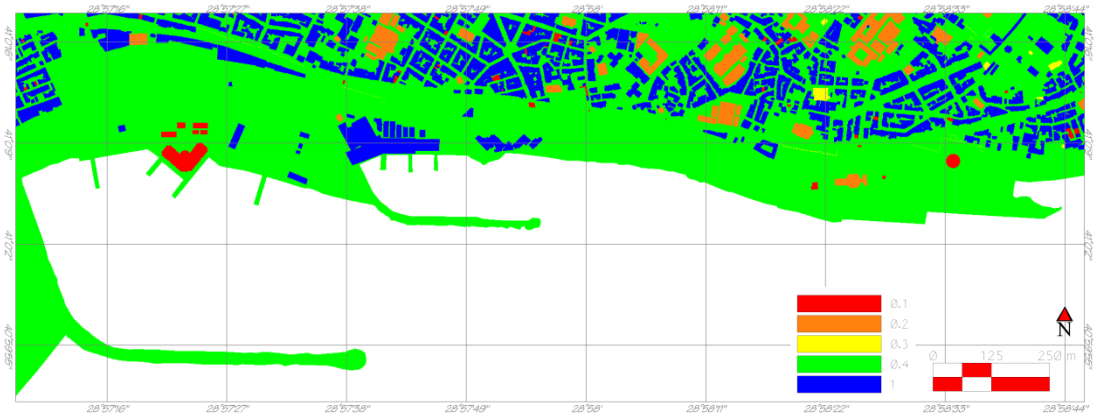

Figure 31: Ranked map of the metropolitan use layer.

A summary of the computed weight and rank values (overall weights) are presented in Table 13.

Table 13: The computed weight and rank values of vulnerability at location.

LAYERS	WEIGHTING	CLASSES	WEIGHT*RANK
Distance from Shoreline	0,4833	< 50	0,04833
		50 - 100	0,09666
		100 - 200	0,14499
		200 - 300	0,28998
		300 - 400	0,43497
		>= 400	0,48330
Geology	0,2917	Quaternary	0,02917
		Miocene	0,08751
		Carboniferous	0,29170
Elevation	0,1208	< 3	0,01208
		3 - 5	0,06040
		5 - 8	0,09664
		>= 8	0,12080
Metropolitan use	0,1042	Extremely Important Places	0,01042
		Assembly Areas	0,02084
		Cultural Heritage	0,03126
		Flat Areas	0,04168
		Buildings	0,10420

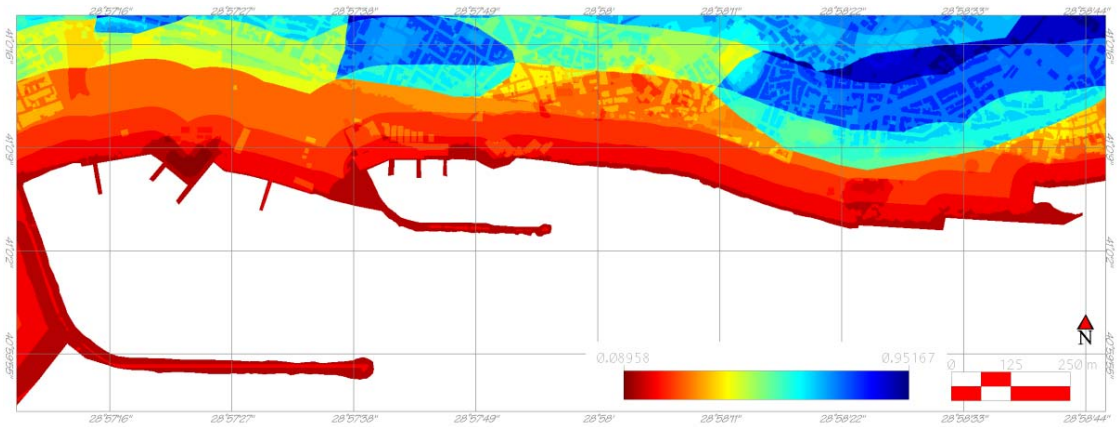

Figure 32: The final map of the locational vulnerability.

3.6 Evacuation Resilience Analysis at Yenikapı Region

Recently, the researches show a key concept in the assessment of tsunami events has been resilience. This section focuses on the evacuation resilience. As previously discussed, there are 4 layers in this group which are distance to building, slope, distance to road network and distance within flat area layers. Multicriteria Decision Making Analysis (MCDA) framework is created to calculate the resilience score for

the evacuation where the places may be exposed to tsunami by manipulation of the input datasets and preparation of the suitable parameter maps.

3.6.1 AHP Analysis for Evacuation Resilience and Production of Resilience Maps

The input dataset are improved and suitable parameter maps/layers are prepared by integrating the MCDA framework for the computation of evacuation resilience score.

It is known that tsunamis are giant waves triggered by mainly earthquakes and/or submarine landslides. These waves come to the near coasts as a series of waves with period changing minutes to hours. However, in this section, while calculating the evacuation resilience score, it is assumed that the waves reach to all places in the study area at the same time; also vertical evacuation is always possible.

The input data and their relevant parameter maps are as follows:

3.6.1.1 Slope Layer

Slope is the one of the important parameters for the tsunami evacuation. It directly affects the velocity of pedestrians to walk over. It will decrease their velocities (Graehl and Dengler, 2008). However, when tsunami propagates inland, gentle slope in the coastal region will make the evacuation easier.

The land slope layer is obtained from the resampled high resolution (1m) DEM (Figure 33). The nearest neighborhood method and 8 bit unsigned integer as raster type are chosen to derive the slope values at each point inside of the study area.

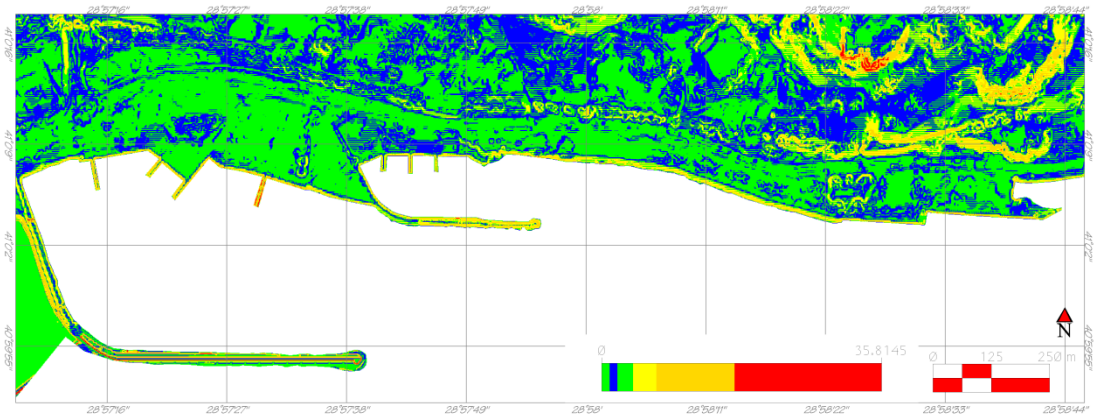

Figure 33: The parameter map of the slope layer.

3.6.1.2 Distance within Flat Areas Layer

In order to produce this layer, the vector form of the metropolitan use layer is used as an input to select the flat areas from their attribute table. Parking places and others (including green fields and public squares) are selected units/polygons from the attribute table. The distance within flat areas of each point can be calculated through rasterization process. The output in raster form will be used in the calculation of evacuation resilience score in the tsunami vulnerability assessment (Figure 34).

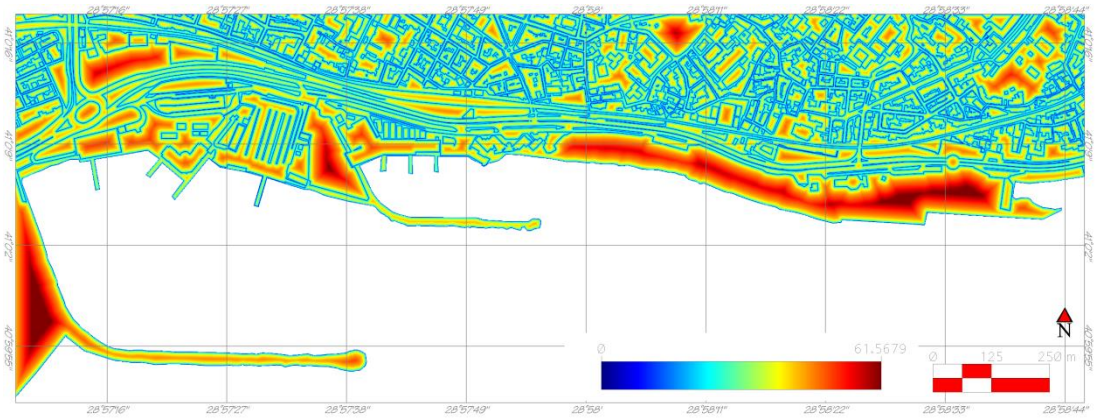

Figure 34: The parameter map of the distance within flat areas layer.

3.6.1.3 Distance to Buildings Layer

The number of the floors of the buildings should be considered while calculation of evacuation resilience of residents. Where vertical evacuation is possible, residents are able to evacuate from the tsunami disaster easily. The risk of injury or death and the loss of life are prevented. However, where the buildings are in the low-rise and the evacuation is not possible in vertical direction, the injury and death will be inevitable (Dominey-Howes and Papathoma, 2007).

According to Mas et al., 2014, the vertical evacuation to high buildings rising over the expected inundation depth in the area is one of the most suitable alternatives in an emergency of a tsunami for plain areas considering the fast arrival of tsunami waves.

The inner conditions of the buildings are important according to some researches, since they believe that the movable object will increase the vulnerability of the buildings. However, in this study, it cannot be considered in the generation of this layer, because of the lack of sufficient available data.

All kind of buildings in the attribute table of the vector form of metropolitan use layer are integrated to generate the parameter layer for buildings. The same method is used like in the generation of the distance within flat areas layer where the polygons representing buildings at the study area are masked and the distance to buildings layer is produced (Figure 35).

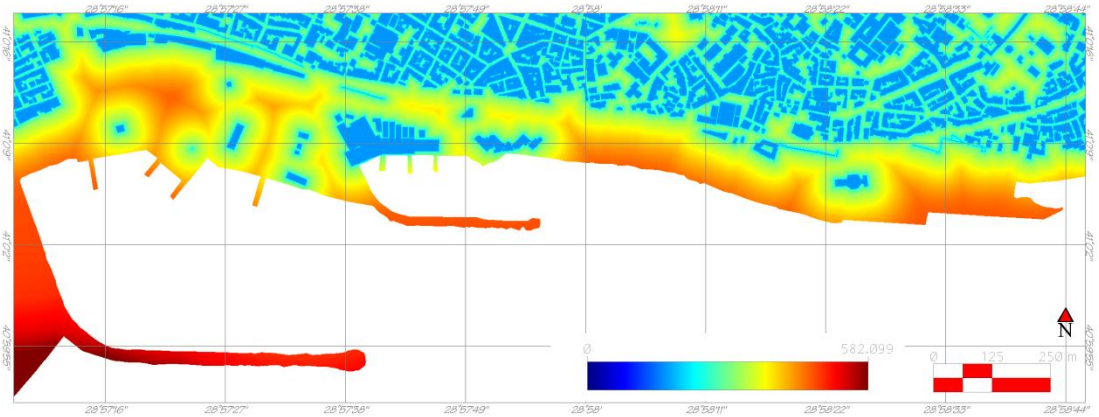

Figure 35: The parameter map of the distance to buildings layer.

3.6.1.4 Distance to Road Networks Layer

The position of the residents in the area during tsunami is critical. Mostly, there is a warning and alert system at the places which have been exposed to tsunamis. The evacuation signs and routes produced by local officials are available in such kind of places. Tsunami evacuation routes/roads guides to the coastal residents to reach the safer locations in case of natural disasters such as earthquake, tsunami, etc. The evacuation signs have been placed along the routes to mark the direction inland or to higher elevations. Depending on the condition of coastal places, there may be more than available direction to find safer areas. If the coastal area does not have any evacuation routes, the main roads should be considered to run away when tsunami approaches inland. In tsunami flooded flat areas, it is very difficult to reach safer places on high ground and away from shoreline. The evacuation time should be shorter as much as possible. For this reason, in this study, the distance to road network layer is regarded in the tsunami vulnerability assessment.

The metropolitan use vector is used to select suburban railway and asphalt roads as potential runaway corridors. The distances to these corridors are calculated with the use of analytical procedures by GIS tools and distance to rad network layer is presented in Figure 36.

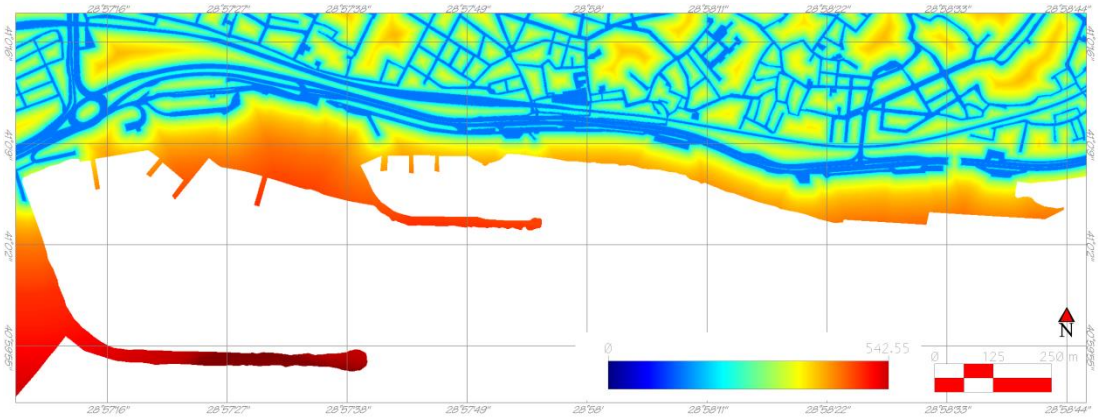

Figure 36: The parameter map of the distance to road networks layer.

3.6.2 Creating AHP Framework and Final Map Production for Evacuation Resilience Score

A score will be computed for evacuation resilience by integrating the parameter maps produced in the previous section (3.6.1) with AHP method of MCDA model. The weight values of the individual 4 layers are determined for by pairwise comparison, depending on Saaty's rating scale (Table 6). The rank values are determined by engineering judgment.

Table 14: The pairwise comparison matrix for calculation of evacuation resilience.

Feature	Slope	Distance within Flat Area	Distance to Building	Distance to Road Network
Slope	**1**	2	1/5	2
Distance within Flat Area	1/2	**1**	1/7	1/3
Distance to Building	5	7	**1**	3
Distance to Road Network	1/2	3	1/3	**1**

The logical explanation of the comparison matrix table while using the assigning values is follows:

• The slope layer has equal-moderate prevalence against the distance within flat areas layer and distance to road network layers, respectively, whereas the distance to building layer has strongly prevalence against the slope layer.

• The distance within flat areas are the least prevalence layer among the other layers, whereas the slope, distance to building and distance to road network layers have equally-moderate, strong and moderate prevalence against the distance within flat areas, respectively.

• The distance to building layer has strong, very strong and moderate prevalence against the slope and distance to road networks layers, respectively.

• The distance to road network layer has moderate prevalence against the distance within flat areas layer, whereas the slope and distance to building layers has equally-moderate and moderate prevalence against the distance to road network layer, respectively.

The weight values are calculated on AHP software by estimating a sufficient consistency ratio (Table 15). As the consistency ratio is obtained as 0.0843 which is less than 0.10, it is compatible to use in AHP method.

Table 15: The computed weight values of the evacuation resilience parameters.

Relative Weights	**By weight order**
Distance to Buildings	0.5808
Slope	0.1830
Distance to Road Networks	0.1647
Distance within Flat Areas	0.0716
Consistency Ratio	0.0843 **(Acceptable!)**

The classes of the 4 layers and their rank values are given in Table 16 to Table 19. The standardization is done for weight and rank values. The evacuation vulnerability maps are also presented in Figure 37 to Figure 40.

Table 16: Classes of the distance to buildings layer.

Distance to Building	Vulnerability Evacuation class	Ranking	Ranking (standardized)
w: 0.5808	< 10	10	1
	10 - 50	9	0.9
	50 - 100	3	0.3
	100 - 250	2	0.2
	>= 250	1	0.1

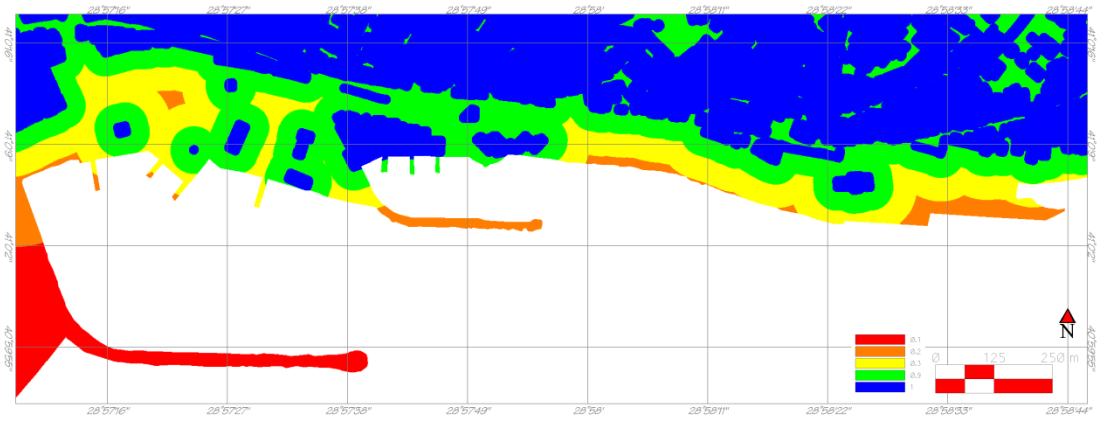

Figure 37: Ranked map of distance to building layer.

Table 17: Classes of the slope layer.

Slope	Vulnerability Evacuation class	Ranking	Ranking (standardized)
w: 0.1830	< 2	10	1
	2 - 4	7	0.7
	4 - 6	4	0.4
	6 - 10	2	0.2
	>= 10	1	0.1

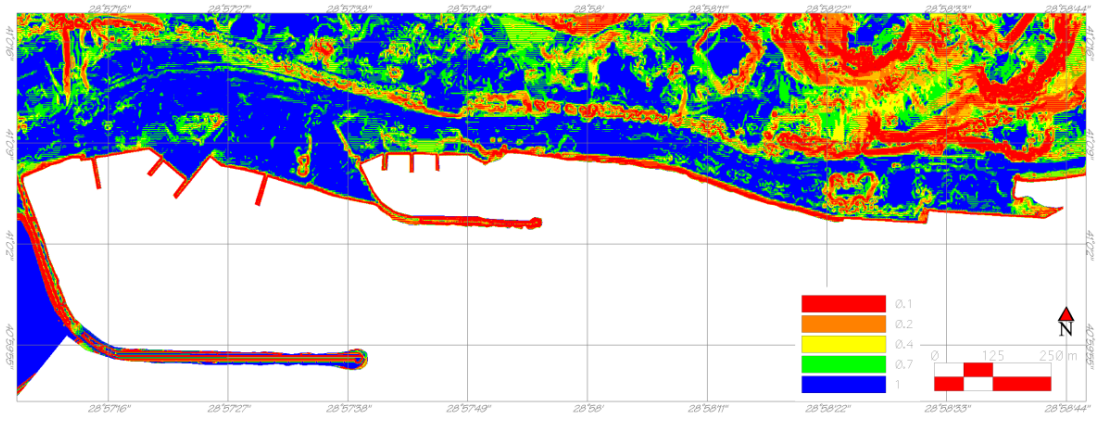

Figure 38: Ranked map of slope layer.

Table 18: Classes of the distance to road networks layer.

Distance to Road Network	Vulnerability Evacuation class	Ranking	Ranking (standardized)
w: 0.1647	< 5	10	1
	5 - 10	9	0.9
	10 - 20	7	0.7
	20 - 50	5	0.5
	50 - 100	3	0.3
	100 - 250	2	0.2
	>= 250	1	0.1

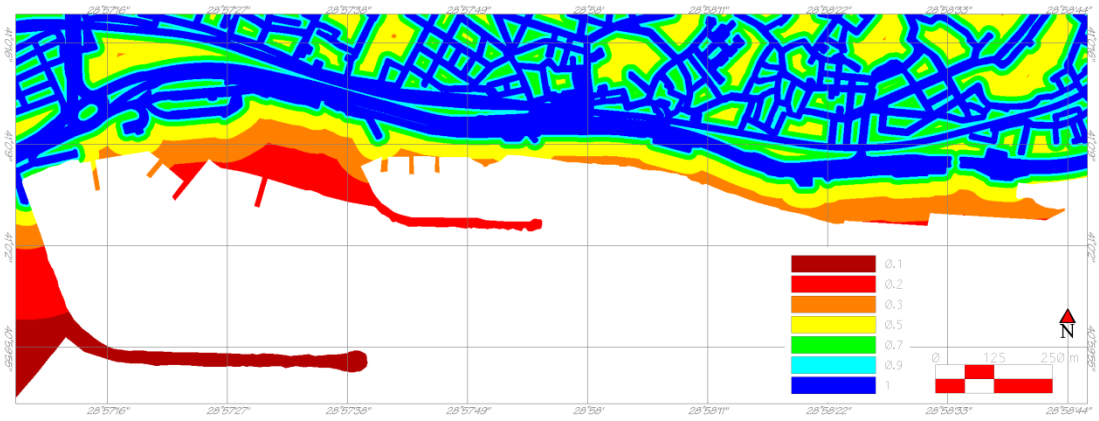

Figure 39: Ranked map of the distance to road networks layer

Table 19: Classes of the distance within flat areas layer.

Distance within Flat Areas	Vulnerability Evacuation class	Ranking	Ranking (standardized)
w: 0.0716	< 10	10	1
	10 - 30	5	0.5
	>= 30	1	0.1

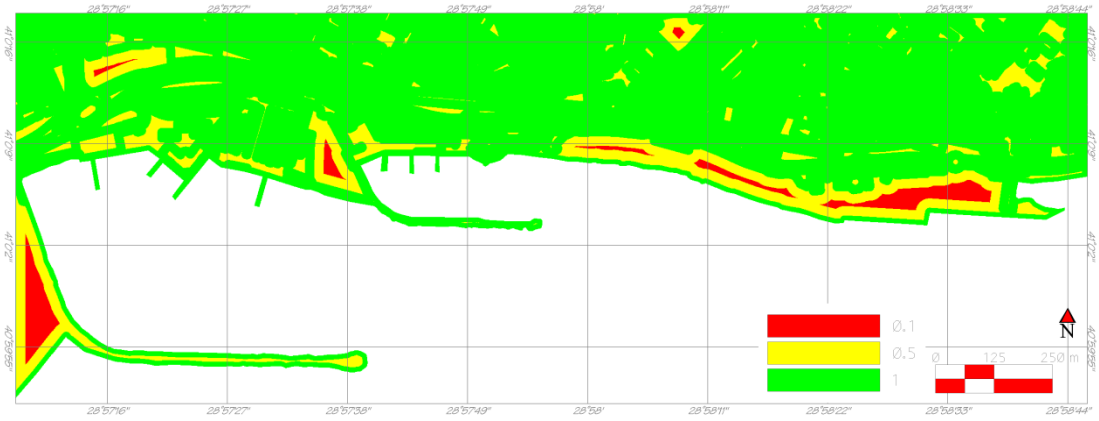

Figure 40: Ranked map of the distance within flat areas layer

A summarized table of the computed weight and rank values for the second group is presented in Table 20.

Table 20: The computed weight and rank values of the evacuation resilience.

LAYERS	WEIGHTING	CLASSES	WEIGHT*RANK
Distance to buildings	**w: 0.5808**	< 10	0,58080
		10 - 50	0,52272
		50 - 100	0,17424
		100 - 250	0,11616
		>= 250	0,05808
Slope	**w: 0.1830**	< 2	0,18300
		2 - 4	0,12810
		4 - 6	0,07320
		6 - 10	0,03660
		>= 10	0,01830
Distance to road networks	**w: 0.1647**	< 5	0,16470
		5 - 10	0,14823
		10 - 20	0,11529
		20 - 50	0,08235
		50 - 100	0,04941
		100 - 250	0,03294
		>= 250	0,01647
Distance within flat areas	**w: 0.0716**	< 10	0,07160
		10 - 30	0,03580
		>= 30	0,00716

The final map of evacuation resilience produced by combination of 4 layers in AHP framework is displayed in Figure 41.

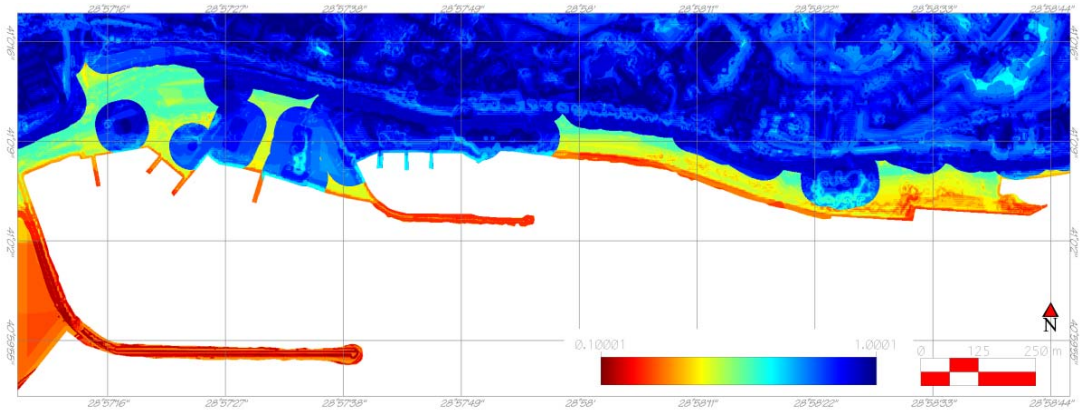

Figure 41: The final map of the evacuation resilience.

By implementing a decision making method, AHP, in GIS environment, the vulnerability score at location and the evacuation resilience score at same location are computed. The output maps and results are presented in this chapter. The results of tsunami numerical modeling are obtained in Chapter 2. These calculated values and produced maps are used to generate tsunami hazard maps.

3.7 Tsunami Hazard Assessment at Yenikapı Region by Presenting the Locational Vulnerability, Evacuation Resilience and Hazard Maps for both Tsunami Sources YAN and PIN

This study presents a new approach for the tsunami vulnerability assessment regarding the association of vulnerability, resilience and numerical computation of Tsunami water depth result. The tsunami hazard assessment is proposed by a new equation which express in Equation 3.1. Haz, H, VL and RE denotes to the tsunami hazard, maximum flow depth in the inundation zone, the vulnerability at location and the evacuation resilience respectively.

$$Haz = log(H + 1) * \left(\frac{VL}{RE}\right) \tag{3.1}$$

When $log1 = 0$, the value of hazard will equal to zero, which means tsunami waves do not reach to these places. The relative hazard can be calculated at the locations where there is a flow depth in inundation zone. The relation of the locational vulnerability and the evacuation resilience are inversely proportional as given in Equation 3.1. The reason is that the overall vulnerability is decreased by the increase of the resilience of evacuation, whereas it increases with any rise in the locational vulnerability. The final maps representing the relative hazard at each location at Yenikapı are generated by using the Equation 3.1 (Figure 42 and Figure 43). These two figures will be discussed in the following section.

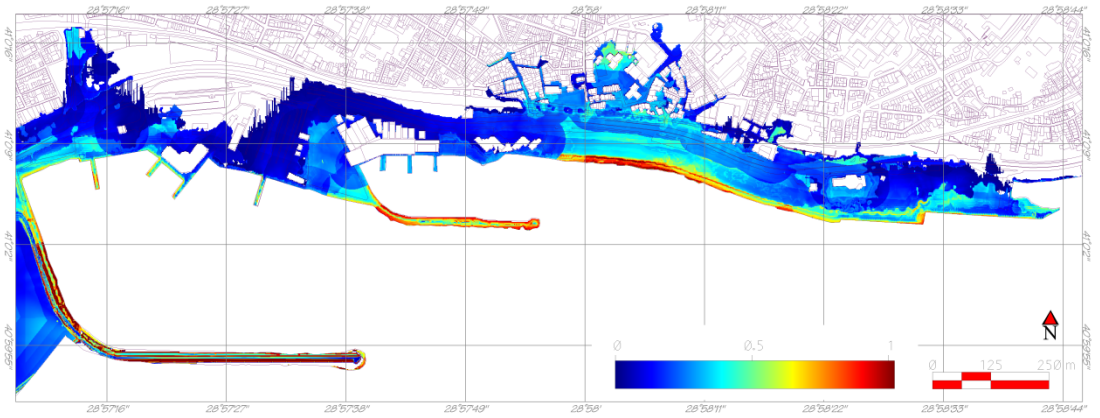

Figure 42: The hazard map derived from the proposed equation (Equation 3.1) by inputting the results of numerical modeling simulations by Prince's Islands normal (PIN) fault.

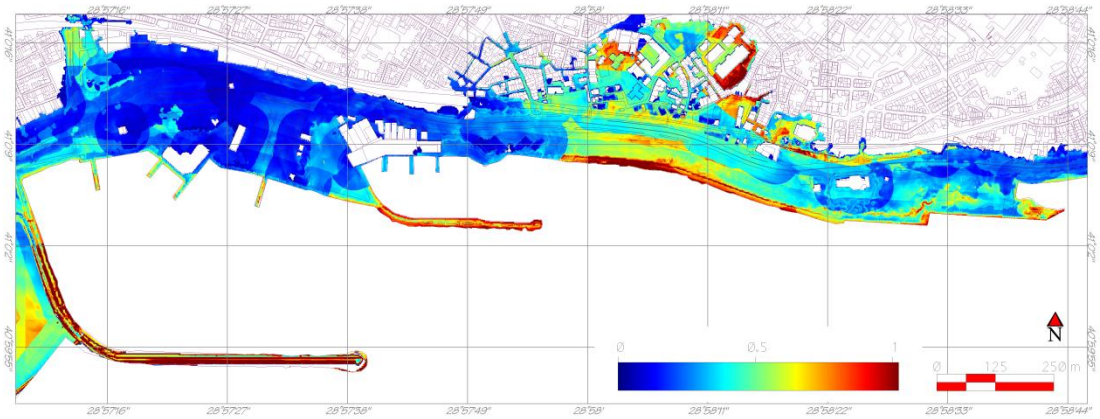

Figure 43: The hazard map derived from the proposed equation (Equation 3.1) by inputting the results of numerical modeling simulations by Yalova normal (YAN) fault.

CHAPTER 4

DISCUSSION

A new approach to tsunami vulnerability assessment by preparation of vulnerability and evacuation resilience maps for Yenikapı coastal region, combining tsunami numerical modeling and GIS-based multicriteria decision making analysis (MCDA), is presented.

In data processing, the topographical data from IMM and bathymetric data from Turkish Navy and GEBCO are enhanced as required in order to input them for high resolution tsunami hazard assessment. GEBCO's bathymetry data is improved with the digitization of the nautical charts. The available vector data combined with the available digital elevation model after data improvement. The high resolution data is processed for simulations of the numerical modeling and tsunami vulnerability and evacuation resilience analyses.

This study can also be performed using 5 m resolution data, but the accuracy of results would not be as reliable as the one computed in this study. Polygons are filled up by 1 m regularly spaced points instead of random points in order to reduce the interpolation effects while increasing the reliability of the data. Because of using the data dated back to 2006, the shoreline is updated to the current shoreline. The resolution of the simulations is sufficient enough for the accurate tsunami hazard assessment.

Both leading elevation and depression waves cause run-up amplification. Nonetheless, the run-up values of the depression waves are higher than the elevation waves because of the accumulation of the accumulation of higher energy (Tadepalli and Synolakis 1996). The maximum flow depths and inundated area based on the

simulations of the PIN and YAN tsunami sources are obtained and the inundation maps are plotted. The inundation maps produced by simulation of these two tsunami sources are compared. According to the generated inundation maps, the tsunami source YAN is found more critical than the tsunami source PIN since it causes higher flow depth and longer inundation distance will be more critical than the other.

The map of locational vulnerability is derived combining the parameter layers by MCDA methods in GIS environments. The most effective parameter layer is observed the distance from shoreline with the weight of 0.4833. The obtained vulnerability score and the plotted map are examined and their similarities are noted. The distance from shoreline layer is dominant as compared to the other parameter layers. Dark red colors represent more vulnerable places comparing with the others. According to the results given in Figure 44a, the safest areas are defined as the locations which are 10 m or less away from any building. The vertical evacuation is possible in the majority of the buildings at Yenikapı. The prefabricated buildings located at behind of the glass-wall building are one-storey structures and their material are not resistant enough against tsunami waves. As it is seen in Figure 44a, there is a color tone difference between the glass wall building and the prefabricated buildings. The reason is that although both are grouped in the extremely important places class; with the effect of the other parameters whereas the glass-wall building is in dark red color, the prefabricated buildings are in red color.

The map of evacuation resilience is plotted as seen in Figure 44b. The buildings are obviously the most resilient places since it is assumed they allow vertical evacuation. However, the breakwaters are the least resilient places because of their closeness to the sea and limited places to run away. The blue colors represent the more resilient places covering the buildings, structures, road networks and flat areas. The less resilient areas for the evacuation are the places near shore at the west of the Yenikapı Fishery Port (Figure 45). The reason is the existence of fish restaurants which are assumed rigid and undamaged. Likewise, depending on the evacuation resilience map, the glass-wall building is represented by blue color as a safer place because it allows to vertical evacuation and locational vulnerability is decreased. When the visit

to the study area, it is noted that the floor numbers of the buildings is mostly more than one at Yenikapı region. The dominant effect of the building layer with the weight of 0.5808 is seen in the evacuation resilience map.

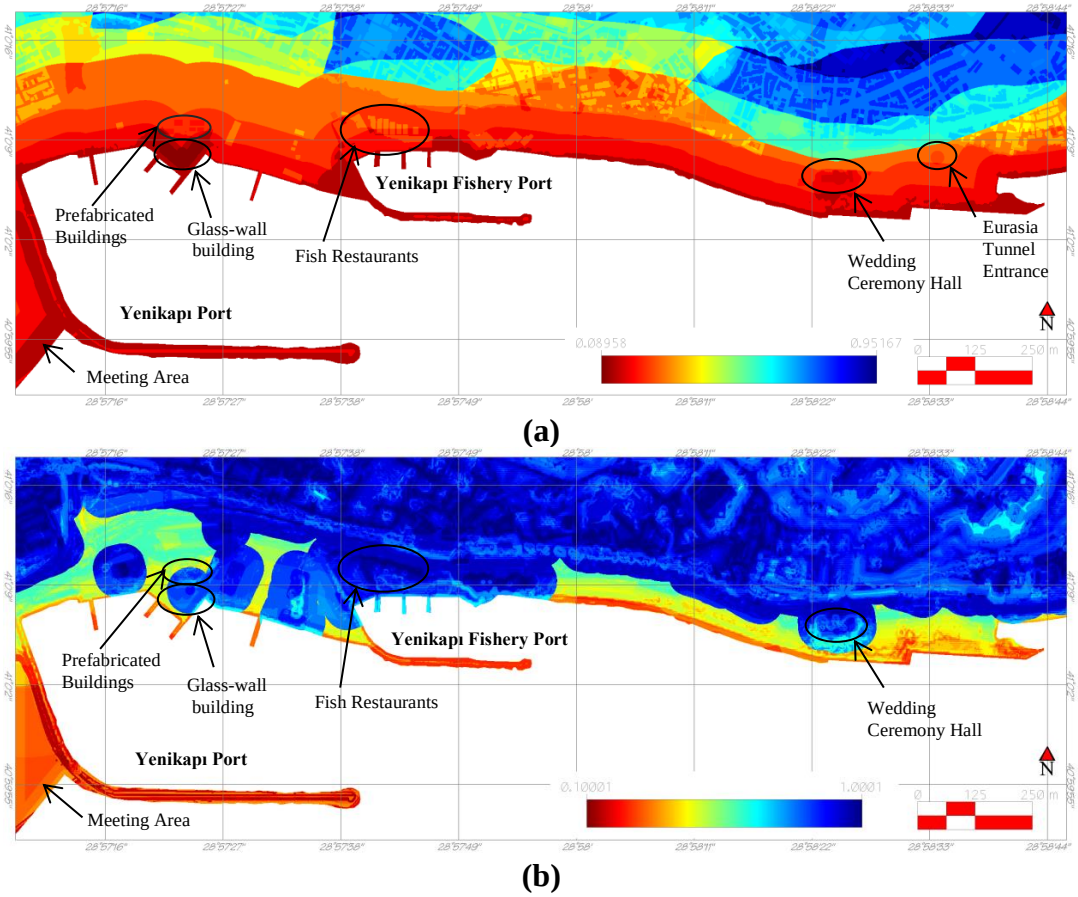

Figure 44: Comparison of locational vulnerability map (a) and evacuation resilience map (b).

Figure 45: A view from the Yenikapı Fishery Port.

The vulnerability and evacuation resilience maps are combined for two critical tsunami sources PIN and YAN separately. For these two sources, the hazard maps are produced using proposed Equation 3.1. The vulnerability and evacuation resilience are relatively defined for each pixel in the study boundary. All individual pixels on representing vulnerability and evacuation resilience level is on scale 0-1. In the hazard maps, blue color represents the relatively safer places, whereas the more hazardous places are red color. White pixels represent the value of zero because of no tsunami arrival (in other words, flow depth is equal to zero). Tsunami hazard increases relatively from blue to red colored areas. By considering the colors in the maps the less hazardous indicative places near shoreline are the İDO-İstanbul Seabus Terminal (ignoring the construction material), the restaurants placed at behind of the Yenikapı Fishery port and the wedding ceremony hall (Figure 46) located at west of the study area nearby shore. The relative vulnerability at east of the Fishery Yenikapı port is maximum because of the existence of the gates of ancient city walls. A small part of meeting area located in the west of the study area is seen an important place due to tsunami impact. The entire meeting area must be considered in tsunami hazard analysis and the necessary precautions should be taken accordingly before facing tsunami disaster.

Figure 46: A view of the wedding ceremony hall at the east side of Yenikapı, nearby shoreline.

The summary of this study is conducted in three steps (Figure 47). The first step covers the tsunami numerical modeling which is estimation of the tsunami source mechanisms in the Sea of Marmara, selection of the study domain as Yenikapı, data processing (enhancement of the available datasets), fine grid simulations, generating high resolution tsunami inundation maps for Yenikapı, respectively. The tsunami inundation maps are produced. In the second step, GIS-based MCDA method is used to gather the geographical data and ease the decision making procedures. GIS tools allow managing a great number of available data by defining spatially and producing tsunami vulnerability maps individually. The outputs of this step are the scores and maps of the vulnerability at location and the evacuation resilience. The third step admits to evaluate hazard in the selected study area, Yenikapı. The new proposed equation (Equation 3.1.) is used in order to produce the hazard maps. The worst case scenario, estimated as YAN, is presented to use for mitigation plan of tsunami disaster.

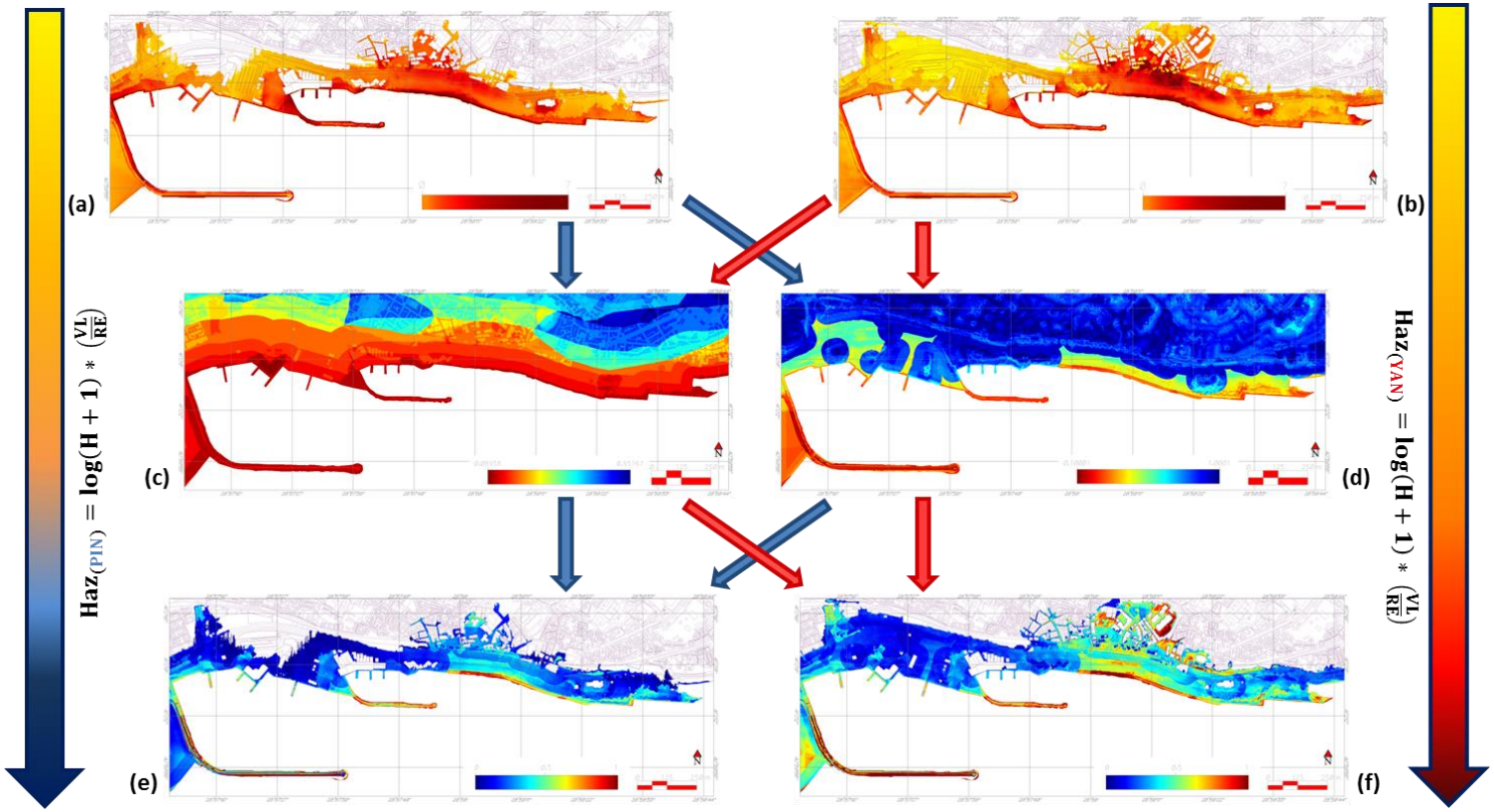

Figure 47: Snapshot of proposed method and used parameters. (a-b) Tsunami inundation map for both PIN and YAN tsunami sources, respectively, (c) Locational vulnerability map, (d) Evacuation resilience map, (e-f) Tsunami hazard maps of PIN and YAN tsunami sources, respectively

This study relies on some assumptions for development of the model. The earthquake is assumed to be a precursor of tsunami which may warn people to consider arrival of a tsunami soon. Even if they are in the most dangerous places, people can move to safer locations which allow best evacuation. It is also assumed that the tsunami waves arrive at the same time at all locations of Yenikapı shoreline in study area (about 2 km portion of Yenikapı shoreline). Another assumption is the duration of inundation which is governed by period of tsunami wave. According to the results of simulations using critical scenario in deterministic approach, the period of tsunami waves is estimated about 10-15 minutes. In the vulnerability analysis, the duration of the tsunami inundation is sufficiently long. The buildings are considered rigid and undamaged by the effect of earthquake and tsunami. Moreover, making pairwise comparison of each layer, it is assumed the vertical escape is possible in every building and the number of the floor is greater than one.

Depending on the simulations, it is understood that the ancient city walls may prevent the tsunami flow through inland. The trend of the tsunami propagation is through the north-west direction of the study area and to the center of the study area behind the Yenikapı Fishery port. For this reason, tsunami moves towards the Fishery port.

One of the critical locations is the prefabricated buildings with 1 floor at shopping area behind the İDO-İstanbul Sea-bus Terminal. Although the prefabricated buildings are represented with lighter color as safer place on the tsunami hazard map, its vulnerability should have been more than the calculated results because of their single storey structures.

The main road in the study area runs parallel along coastline, which is not convenient for evacuation when a tsunami occurs.

The places assigned as the extremely important places (the prefabricated buildings, the glass wall building, the entrance of the Eurasia Undersea Highway Tunnel, ruins, the entrance of pedestrian underpasses, gas stations, electricity transformers) are relatively more vulnerable by considering the locational and evacuation

vulnerabilities.

Some car underpasses on the main road at Yenikapı cause penetration of the water inland, which would probably make the evacuation harder (Figure 48).

Figure 48: Two different views from the different entrances of car underpasses.

CHAPTER 5

CONCLUSION

In this study, a new approach is applied to define tsunami vulnerability parameters and a new model for high resolution tsunami vulnerability assessment based on tsunami numerical modeling and GIS-based multicriteria decision making analysis is proposed.

According to results obtained from the above summarized studies the main concluding remarks are listed below.

1. There is tsunami potential in the Sea of Marmara and tsunami hazard analysis including detailed vulnerability and hazards analysis are necessary. A new approach is presented and tested with the case study for Yenikapı region in İstanbul.

2. Determination of the tsunami sources affecting the study area is one of the main requirements of tsunami numerical modeling. These sources must be analyzed and compared to determine the critical deterministic tsunami scenarios for the study area. Valid and verified numerical model is necessary for detailed computation of near shore and over land tsunami parameters (such as inundation, maximum positive amplitudes, flow depths and maximum currents). The inundation map including the flow depth (depth of overland tsunami flow) must be calculated.

3. High resolution bathymetry, topography and the vector data of metropolitan use are the main requirements for the proposed, detailed and proper vulnerability, resilience and hazard analyses.

4. The flow depth at Yenikapı exceeds 6m at the near shore and the location

between the historical city walls behind the Yenikapı Fishery port and the shoreline because of the accumulation of water volume. The inundation distance reaches 200 m inland depending on the YAN source simulations by tsunami numerical modeling.

5. Vulnerability and evacuation resilience mapping are conducted and inundation is assessed using GIS and MCDA. AHP method is used to assign weight values to parameter layers and rank values to the classes. Eight parameter layers (distance from shoreline, geology, elevation, metropolitan use; slope, distance from buildings, distance to road network, distance within flat areas) related with vulnerability and resilience are defined and four of which are used for locational vulnerability analysis. The other four are used in evacuation resilience analysis. A MCDA model, AHP, is applied on the parameter maps to obtain the maps of vulnerability at location and evacuation resilience for Yenikapı region. In the calculation of the vulnerability score at location, the distance from shoreline layer is the most influential layer depending on its weight value (0.4833), whereas the least influential layer is found metropolitan use layer based on its weigh value (0.1042). The most effective parameter on evacuation resilience is found the distance to building layer with the value of 0.5808, whereas the least effective is the distance within flat areas layer with the value of 0.0716.

6. Two tsunami hazard maps are generated by association of the results of numerical models of two different sources, and GIS-based MCDA method results (vulnerability map and evacuation resilience map) in the new proposed tsunami hazard map equation (Equation 3.1). For Yenikapı region, the tsunami source YAN is selected as the most critical source, since the results of the simulations of YAN give higher flow depth and longer inundation distance. Therefore, the hazard map obtained by the combination of the results of YAN source simulations, vulnerability at location and the evacuation resilience is presented to be considered in the tsunami disaster mitigation system.

For the future studies, there are some suggestions to be considered which are listed as followings:

1. Depending on the locational vulnerability map, some structures/locations categorized as extremely important places (prefabricated buildings, gas station, electricity transformer, pedestrian underpasses, glass wall building, the entrance of the Eurasia Undersea Highway Tunnel, ruins) are less vulnerable than it is expected. The places defined as extremely important would be analyzed separately instead of evaluating them into the overall vulnerability. By this way, it would be possible to avoid underestimation of their importance.

2. Another suggestion is that density layer can be generated for tsunami hazard assessments if the number of citizens in the selected area is known. Thus, the tsunami vulnerability assessments would be performed in detail and possible calamities and/or the intensity of the tsunami would be predicted and the required precautions would be taken.

3. For the tsunami vulnerability assessments, the roads would be divided into the evacuation roads. Thus, the shortest distance would be calculated to move away from the tsunamis. The roads can be evaluated by separately depending on their width and the direction to move to the safer places.

4. Velocity of the waves would be used in the tsunami vulnerability assessment and the vulnerability of the buildings and/or human-built structures would be computed.

REFERENCES

Akkargan, Ş., Alpar, B., 2000. Active faults in izmit Bay and Adalar region; 1894 earthquake (in Turkish). Jeofizik 14, 3-14.

Alexander, D.: 2000, Confronting catastrophe: new perspectives on natural disasters. Terra Publishing, 282 pp.

Alpar, B., Yaltırak, C., 2000a. Anatomy of the North Anatolian Fault in the İzmit Bay and related e¡ects of 17 August 1999 Earthquake. In: Tatar, O., Kavak, K.Ş., Özden, S. (Eds.), Articles of the Active Tectonic Research Group, III Workshop, pp. 51-58.

Alpar, B., Yaltırak, C., 2000b. Tectonic setting of the Marmara Sea. NATO Advanced Research Seminar, Integration of Earth Sciences on the 1999 Turkish and Greek Earthquakes and Needs for Future Cooperative Research, Abstracts, 14-17 May 2000. İstanbul, pp. 9-10.

Altınok, Y., Alpar, B., Ersoy, Ş., Yalciner, A.C., 1999. Tsunami generation of the Kocaeli Earthquake (August 17th 1999) in the İzmit Bay: coastal observations, bathymetry and seismic data. Turk. J. Mar. Sci. 5, 131-148.

Altınok, Y., Tinti, S., Alpar, B., Yalciner, A.C., Ersoy, Ş., Bortolucci, E., Armigliato, A., 2001b. The tsunami of August 17, 1999 in İzmit Bay. Nat. Hazards 24, 133-146.

Altınok, Y., Alpar, B., Özer, N., & Aykurt, H. (2011). Revision of the tsunami catalogue affecting Turkish coasts and surrounding regions. Natural Hazards and Earth System Science, 11(2), 273–291.

Altınok, Y., Ersoy, Ş., 2000. Tsunamis observed on and near the Turkish coast. Nat. Hazards 21, 185-205.

Altınok, Y., B. Alpar and C. Yaltirak (2003) Sarkoy-Murefte 1912 Earthquake's Tsunami, extension of the associated faulting in the Marmara Sea, Turkey. Journal of Seismology 7: pp. 329-346.

Altınok, Y. (2006). Turkiye ve Cevresinde Tarihsel Tsunamiler. Turkiye Muhendislik Haberleri, pp.25-32.

Ambraseys, N.N., 1962. Data for the investigation of the seismic sea-waves in the Eastern Mediterranean. Bull. Seism. Soc. Am. 52, 895-913.

Ambraseys, N.N., Finkel, C.F., 1991. Long term seismicity of İstanbul and of the Marmara Sea region. Terra Nova 3, 527-539.

Antonopoulos, A., 1978. Contribution to the knowledge of tsunamis in the Eastern Mediterranean from ancient times until the recent. Ann. Geol. Pays Hell. ser. TXXIX/2, 740-757.

Ayca, A., (2012). Development of A Web GIS-Based Tsunami Inundation Mapping Service; A Case Study For Marmara Sea Region. M.S. Thesis METU, Ankara, Turkey

AYTORE B., CANKAYA C. Z., YALÇINER A. C., SUZEN M. L., ZAYTSEV A., 2014, High Resolution Data Processing and Tsunami Assessment and Applications to Ports In the Sea of Marmara, METSZ, International Workshop on Mega Earthquakes and Tsunamis in Subduction Zones: Forecasting Approaches and Implications for Hazard Assessment, 6-8 Oct 2014, Rhodes, Greece.

Batur, A., 1994. Bir depremin yüzyıl dönümü. İstanbul Derg. 10, 24-33.

Bozkurt, E. : Neotectonics of Turkey - a synthesis, Geodinamica Acta, 14(1–3), 3–30, 2001.

Cartwright, J. H. E. and Nakamura, H., 2008. Tsunami: a history of the term and of scientific understanding of the phenomenon in Japanese and Western culture. Notes and Records of the Royal Society, 62(2): 151-166.

Cheung, K. F., Phadke, A. C., Wei, Y., Rojas, R., Douyere, Y., Martino, C. D., Houston, S. H., Liu, P., Lynett, P. J., Dodd, N., Liao, S., and Nakazaki, E.: 2003, Modelling of storm induced coastal flooding for emergency management, Ocean Eng. 30, 1353–1386.2

Dalgıç S., Turgut M., Kuşku İ., Coşkun İ.,Coşgun T., 2009 İstanbul'un Avrupa Yakasındaki Zemin ve Kaya Koşullarının Bina Temellerine Etkisi, Uygulamalı Yer Bilimleri (2), 47-70.

Dall'Osso, F., Gonella, M., Gabbianelli, G., Withycombe, G. and Dominey-Howes, D.: "Assessing the vulnerability of buildings to tsunami in Sydney". Natural Hazards and Earth System Sciences (NHESS), 9, 2015–2026, 2009a.

Dall'Osso, F., Gonella, G., Gabbianelli, G., Withycombe, G., and Dominey-Howes, D.: The vulnerability of buildings to tsunami in Sydney, Nat. Hazards Earth Syst. Sci., in review, 2009b.

Dall'Osso F., Maramai, A., Graziani, L., Brizuela, B., Cavalletti, A., Gonella, M., Tinti, S., 2010 Applying and validating the PTVA-3 Model at the Aeolian Islands, Italy: assessment of the vulnerability of buildings to tsunamis, Nat. Hazards Earth Syst. Sci.

Dilmen D.I., S. Kemec, A.C. Yalciner, S. Duzgun, A. Zaytsev, 2014

Development of Tsunami Inundation Map in Detecting Tsunami Risk in Gulf of Fethiye, Turkey, Pure Appl. Geophys. Springer Basel

Dominey-Howes, D., Papathoma, M. (2007). Validating a Tsunami Vulnerability Assessment Model (the PTVA Model) Using Field Data from the 2004 Indian Ocean Tsunami. Natural Hazards, 40(1), 113–136.

Dominey-Howes, D., Bird D.K., Gisladottir G., 2010 Volcanic risk and tourism in southern Iceland: Implications for hazard, risk and emergency response education and training, Journal of Volcanology and Geothermal Research, 189, 33-48

Erel, L., Eriş, K. K., Akçer, S., Biltekin D., Beck, C. ve Çağatay M. N., 2009. Bayrampaşa (Lykos) Deresi Havzası ve Ağzındaki Yenikapı (Theodosius) Limanı Kıyı Alanındaki (Marmara Denizi) Değişim Süreçleri. 62. Türkiye Jeoloji Kurultayı, 13-17 Nisan 2009, MTA -Ankara, 58-59.

Fischer, T., Alvarez, M., Dela Llera, J., and Riddell, R.: 2002, An integrated model for earthquake risk assessment of buildings, Eng. Struct. 24, 979–998.

Gambolati, G., Teatini, P., and Gonella, M.: 2002, GIS simulations of the inundation risk in the coastal lowlands of the northern Adriatic Sea, Mathem. Comput. Model. 35, 963–972.

Graehl, N.A., Dengler, L., 2008. Using a GIS to model tsunami evacuation times for the community of Fairhaven, California, Eos Trans. AGU, 89(53), Fall Meet.Suppl., Abstract OS43D-1324

Gürer Ö.F., Kaymakçı N., Çakır Ş., Özburan M., 2002, Neotectonics of the southeast Marmara region, NW Anatolia, Turkey, Journal of Asian Earth Sciences, 21, 1041-1051.

Hebert, H., F. Schindele, Y. Altınok, B. Alpar and C. Gazioglu 2005 Tsunami hazard in the Marmara Sea (Turkey): a numerical approach to discuss active faulting and impact on the Istanbul coastal areas. Marine Geology, 215, 23-43.

Heidarzadeh M., Pirooz M.D., Zaker N.H., Yalciner A.C., Mokhtari M., Esmaeily A. (2008) Historical tsunami in the Makran Subduction Zone off the southern coasts of Iran and Pakistan and results of numerical modeling, Ocean Engineering, 35, 774-786.

Heidarzadeh M., Krastel S., Yalciner A. C., 2013 "Chapter 43, The State-of-the-Art Numerical Tools for Modeling Landslide Tsunamis: A Short Review", S. Krastel et al. (eds.), Submarine Mass Movements and Their Consequences, Advances in Natural and Technological Hazards Research 37.

IMM, O. a. (2008). Project report on simulation and vulnerability analysis of Tsunamis affecting the İstanbul Coasts. İstanbul: OYO Int. Co. (Japan) for İstanbul Metropolitan Municipality (IMM)

IMM, 2015, Jeoloji Haritası, retrieved from http://www.ibb.gov.tr/tr-TR/SubSites/DepremSite/Documents/EK2_Jeoloji_Haritasi_1440x910_25000_300DPI.pdf, last visited on September, 2014

Janssen, R., 1992, Multiobjective Decision Support for Environmental Management, Kluwer Academic Publishers, 232 p.

Jenkins, L. : 2000, Selecting scenarios for environmental disaster planning, Eur. J. Oper. Res. 121, 275–286. Papadopoulos, G.A., Chalkis, B.J., 1984. Tsunamis observed in Greece and the surrounding area from antiquity to the present times. Mar. Geol. 56, 309-317.

Kaiser G., Scheele L, Kortenhaus A., Lovholt F., Römer H., Leschka S., 2011 The influence of land cover roughness on the results of high resolution tsunami modeling, Natural Hazards and Earth System Sciences, 11, 2521-2540.

Kolat, Ç. (2004). Geographical Information Systems Based Microzonation Map of Eskişehir Downtown Area. M.S. Thesis METU, Ankara, Turkey

Kolat, Ç., Doyuran, V., Ayday, C., & Lütfi Süzen, M. (2006). Preparation of a geotechnical microzonation model using Geographical Information Systems based on Multicriteria Decision Analysis. Engineering Geology, 87(3-4), 241-255.

Kolat Ç., Ulusay R., Süzen M.L., 2012 Development of geotechnical microzonation model for Yenisehir (Bursa, Turkey) located at a seismically active reigon, Engineering Geology, 127, 36-53.

Koshimura, S., Namegaya, Y., & Yanagisawa, H., 2009. Tsunami Fragility: A New Measure to Identify Tsunami Damage. Journal of Disaster Research, 4(6).

Kuran, U., Yalciner, A.C., 1993. Crack propogations earthquakes and tsunamis in the vicinity of Anatolia. In: Tinti, S. (Ed.), Fifteenth International Tsunami Symposium, 1991, Tsunamis in the World. Kluwer, Dordrecht, pp. 159-175.

Malczewski, J.,1999, GIS and Multicriteria Decision Analysis, John Willey and Sons Inc., 392 p.

Malinowska A.A., Dziarek K.,2014 Modelling of cave-in occurrence using AHP and GIS, Natural Hazards and Earth System Sciences, 14.

Marshall, K.T., Oliver, R.M., 1995, Decision Making and Forecasting, McGraw-Hill, Inc., 407 p.

Mas E., Adriano B., Koshimura S., Imamura F., Kuroiwa H.J., Yamazaki F., Zavala C., Estrada M, 2014, Identifying Evacuees' Demand of Tsunami Shelters using Agent Based Simulation

Mercier, J.L., Sorel, D., Vergely, P., 1989. Extensional tectonic regimes in the

Aegean basins during the Cenozoic. Basin Res. 2, 49-71.

Modica G., Laudari L., Barreca F., Fichera C.R., 2014 A GIS-MCDA Based Model for the Suitability Evaluation of Traditional Grape Varieties: The Case Study of 'Mantonico' Grape (Calabria, Italy), International Journal of Agricultural and Environmental Information System, 5(3).

NAMI DANCE (2013), Tsunami Numerical Modeling NAMI DANCE Manual, http://namidance.ce.metu.edu.tr/pdf/NAMIDANCE-version-5-9-manual.pdf

Niaraki M.J., Malczewski, J., 2014 The decision task complexity and information acquisition strategies in GIS-MCDA, International Journal of Geographical Information Science.

Omira, R., Baptista, M. a., Miranda, J. M., Toto, E., Catita, C., & Catalão, J.,2010 Tsunami vulnerability assessment of Casablanca-Morocco using numerical modelling and GIS tools. Natural Hazards, 54(1), 75–95.

Özçiçek, B., 1996. 18 Eylül 1963 Doğu Marmara depreminin etudü. Jeofizik 1, 69-78.

Özdemir K.K. (2014). Database Development For Tsunami Information System. M.S. Thesis METU, Ankara, Turkey

Özer C., Yalciner A.C.,2011 Sensitivtiy Study of Hydrodynamic Parameters During Numerical Simulations of Tsunami Inundation, Pure and Applied Geophysics.

Özer C., Yalciner A.C., Zaytsev A., 2014. Investigation of Tsunami Hydrodynamic Parameters In Inundation Zone With Different Structural Layout, Pure and Applied Geophysics.

Özgül N., Özcan İ., Akmeşe İ., Üner K., Bilgin İ., Korkmaz R., Yıldırım Ü., Yıldız Z., Akdağ Ö., Tekin M., 2011 , İstanbul İl Alanının Jeolojisi, İstanbul Büyükşehir Belediyesi, İstanbul

Öztin, F., Bayülke, N., 1991. Historical earthquakes of İstanbul, Kayseri, Elazığ. Proceedings of the Workshop on Historical Seismicity and Seismotectonics of the Mediterranean Region, 10-12 Oct. 1990. Turkish Atomic Energy Authority, Ankara, pp. 150-173.

Öztin, F., 1994. 10 Temmuz 1894, İstanbul Depremi Raporu.T.C. Bayındırlık ve İskan Bakanlığı, Afet İşleri Genel Müdürlüğü, Deprem Araştırma Dairesi, Ankara.

Papadopoulos, G.A., Chalkis, B.J., 1984. Tsunamis observed in Greece and the surrounding area from antiquity to the present times. Mar. Geol. 56, 309^317.

Papathoma, M. 2003. Assessing tsunami vulnerability using GIS with special

reference to Greece. Unpublished PhD thesis, Coventry University (UK), 290 pp.

Papathoma, M., Dominey-Howes, D., 2003 Tsunami vulnerability assessment and its implications for coastal hazard analysis and disaster management planning , Gulf of Corinth , Greece. Natural Hazards and Earth System Science, 3, 733–747.

Papathoma, M., Dominey-Howes, D., Zong, Y., and Smith, D.: 2003, Assessing tsunami vulnerability, an example from Heraklion, Crete, Nat. Hazards Earth Syst. Sci. 3, 377–389

Parsons, T., Stein, R.S., Barka, A.A., Dieterich, J.H., 2000. Heightened odds of large earthquakes near İstanbul; an interaction-based probability calculation. Sci. Mag. April 28, 2000, 661-665.

Rikalovic, A., 2014, Cosic I., and Lazarevic, D., 2014. GIS Based Multi-Criteria Analysis for Industrial Site Selection. Procedia Engineering 69, 1054 – 1063

Rikavolic A., Cosic I., Lazarevic D.,2014 GIS Based Multi-Criteria Analysis for Industrial Site Selection, Procedia Engineering, 69, 1054-1063.

Saaty. T.L., 1980, The Analytic Hierarchy Process, McGraw-Hill.

Saaty, T.L., 1990, How to make a Decision: The Analytic Hierarchy Process, European Journal of Operational Research, 48, pp 9-26.

Saaty, T.L., 2003, Decision Making with the AHP: Why is the Principal Eigenvector Necessary, European Journal of Operational Research, 145, pp 85-91.

Santos, A., Tavares, A. O., & Emidio, A.,2014 Comparative tsunami vulnerability assessment of an urban area: An analysis of Setúbal city, Portugal. Applied Geography, 55, 19–29.

Shebalin, N.V., Karnik, V., Hadzievski, D., 1974. Catalogue of Earthquakes. Unesco, Skopje.

Smith, A.D., Taymaz, T., Oktay, F., Yüce, H., Alpar, B., Başaran, H., Jackson, J.A., Kara, S., Şimşek, M., 1995. High-resolution seismic profilng in the Sea of Marmara (Northwest Turkey): Late Quaternary sedimentation and sea-level changes. Geol. Soc. Am. Bull. 107, 923-936.

Soysal, H., 1985. Tsunami (deniz taşması) ve Türkiye kıyılarını etkileyen tsunamiler. Istanb. Univ. Bull. Mar. Sci. Geogr. 2, 59-67.

Soysal, H., Sipahiogfllu, S., Kolçak, D., Altınok, Y., 1981. Turkiye ve Çevresinin Tarihsel Deprem Kataloğu (MO 2100-MS 1900), TUBITAK project Tbag 341. İstanbul.

Straub, C., Kahle, H.G., 1997. Recent crustal deformation and strain accumulation in the Marmara Sea region, NW Anatolia, inferred from repeated GPS measurements. In:Schindler, C., Pfister, M. (Eds.), Active Tectonics of Northwestern Anatolia-The Marmara Poly-Project. VdF Hochschulverlag AG der ETH, Zurich, pp. 417-447.

Şener, B. (2004). Landfill Site Selection by Using Geographic Information Systems. M.S. Thesis METU, Ankara, Turkey

Şener, B., Süzen M. L., and Doyuran, V. 2006. Landfill site selection by using geographic information systems. Environ Geol 49, 376–388.

Şengör, A.M.C., Demirbağ, E., Tüysüz, O., Kurt, H., Görür, N., Kuşçu, İ., 1999. İzmit Körfezinin deniz altında kalan resminin jeolojik yapısı. Cumhuriyet Bilim Teknik 14 Aralık, 1999, pp. 17-18.

Tadepalli S., Synolakis C.E., 1996, Model for the leading waves of tsunamis, Physical Review Letters 77(10), 2141.

Tammi, I., Kalliola R. (2013) Spatial MCDA in marine planning: Experiences from the Mediterranean and Baltic Seas, Marine Policy 48, 73-83

Tarbotton, C., Dominey-Howes, D., Goff, J. R., Papathoma-Kohle, M., Dall'Osso, F., & Turner, I. L., 2012 GIS-based techniques for assessing the vulnerability of buildings to tsunami: current approaches and future steps. Geological Society, London, Special Publications, 361(1), 115–125.

Thill, J.C., 1999, Spatial Multicriteria Decision Making and Analysis – A Geographical Information Sciences Approach, Ashgate Publishing Company, 377p.

Tufekci, S.: 1995, An integrated emergency management decision support system for hurricane emergencies, Saf. Sci. 20, 39–48

URL-1: Avrupa Yakası Güneyi Mikrobölgeleme Projesi, http://www.ibb.gov.tr/tr-TR/SubSites/DepremSite/Pages/AvrupaYakasiGuneyiMikrobolgelemeProjesi.aspx, last visited on January, 2015

URL-2: Tsunami Risk And Strategies for the European Region (TRANSFER), Deliverable 5.4, http://www.transferproject.eu/, last visited on December, 2014

USGS, 2015, Life of a tsunami, http://walrus.wr.usgs.gov/tsunami/basics.html, last visited on January, 2015.

Wisner, B., Blaikie, P., Cannon, T. and Davis, I.: 2004, At risk: natural hazards, people's vulnerability and disasters. Routledge, 2nd edn, 284 pp. http://www.asiantsunamivideos.com [accessed 11th May 2005.].

Yalciner, A. C., Alpar, B., Altınok, Y., Özbay, İ., & Imamura, F., 2002 Tsunamis in The Sea of Marmara Historical Documents for The Past Models for The Future. Marine Geology, 190, 445–463.

Yalciner, A.C., Karakuş, H., Özer, C. and Özyurt, G. (2005) Short Courses on Understanding the Generation, Propagation, Near and Far-Field Impacts of TSUNAMIS and Planning Strategies to Prepare for Future Events, Course Notes in Kuala Lumpur (METU Civil Eng. Dept. Ocean Eng. Res. Center, 2005)

Yalciner A.C. , Gülkan P. , Dilmen D.I. , Aytöre B. , Ayca A. , İnsel İ. , Zaytsev A. , 2014 Evaluation of tsunami scenarios for western Peloponnese,Greece, Bollettino di Geofisica Teorica ed Applicata 55(2), 485-500.

Yalciner A.C., Zahibo N., Pelinovsky E., İnsel İ., Dilmen D.I , Zaytsev A., Özer C., 2010 Understanding the Possible Effects of Near and Far Field Tsunamis on Lesser Antilles By Numerical Modeling, The Open Oceanography Journal, 3, 67-69

Yalciner A. C., Suppasri A., Mas E., Kalligeris N., Necmioglu O., Imamura F., Ozer C., Zaytsev A., Ozel M. N., Synolakis C., (2011), Field Survey on the Coastal Impacts of March 11, 2011 Great East Japan Tsunami, Submitted to Journal of Pure and Applied Geophysics, (in review)

Yaltırak, C., Alpar, B., Sakınç M., Yüce, H., 2000. Origin of the Strait of Canakkale (Dardanelles): regional tectonics and the Mediterranean - Marmara incursion. Mar. Geol. 164, 139-156, with erratum 167, 189-190.